ELSEVIER

Advances in Colloid and Interface Science 119 (2006) 17 – 33

ADVANCES IN COLLOID AND INTERFACE SCIENCE

www.elsevier.com/locate/cis

Mass transport in micellar surfactant solutions: 2. Theoretical modeling of adsorption at a quiescent interface

K.D. Danov [a], P.A. Kralchevsky [a,*], N.D. Denkov [a], K.P. Ananthapadmanabhan [b], A. Lips [b]

[a] *Laboratory of Chemical Physics and Engineering, Faculty of Chemistry, University of Sofia, 1164 Sofia, Bulgaria*
[b] *Unilever Research and Development, Trumbull, CT 06611, USA*

Available online 23 November 2005

Abstract

Here, we apply the detailed theoretical model of micellar kinetics from part 1 of this study to the case of surfactant adsorption at a quiescent interface, i.e., to the relaxation of surface tension and adsorption after a small initial perturbation. Our goal is to understand why for some surfactant solutions the surface tension relaxes as inverse-square-root of time, $1/t^{1/2}$, but two different expressions for the characteristic relaxation time are applicable to different cases. In addition, our aim is to clarify why for other surfactant solutions the surface tension relaxes exponentially. For this goal, we carried out a computer modeling of the adsorption process, based on the general system of equations derived in part 1. This analysis reveals the existence of four different consecutive relaxation regimes (stages) for a given micellar solution: two exponential regimes and two inverse-square-root regimes, following one after another in alternating order. Experimentally, depending on the specific surfactant and method, one usually registers only one of these regimes. Therefore, to interpret properly the data, one has to identify which of these four kinetic regimes is observed in the given experiment. Our numerical results for the relaxation of the surface tension, micelle concentration and aggregation number are presented in the form of kinetic diagrams, which reveal the stages of the relaxation process. At low micelle concentrations, "rudimentary" kinetic diagrams could be observed, which are characterized by merging of some stages. Thus, the theoretical modeling reveals a general and physically rich picture of the adsorption process. To facilitate the interpretation of experimental data, we have derived convenient theoretical expressions for the time dependence of surface tension and adsorption in each of the four regimes.

Keywords: Micellar surfactant solutions; Fast and slow micellization processes; Adsorption kinetics of surfactants; Dynamic surface tension; Diffusion in micellar surfactant solutions

Contents

* Corresponding author. Tel.: +359 2 962 5310; fax: +359 2 962 5438.
E-mail address: pk@lcpe.uni-sofia.bg (P.A. Kralchevsky).

0001-8686/$ - see front matter © 2005 Elsevier B.V. All rights reserved.
doi:10.1016/j.cis.2005.09.003

1. Introduction

In the first part of this study [1], we proposed a theoretical model, which generalizes previous models of micellization kinetics in the following aspects. First, we did not apply the simplifying assumption that the width of the micellar peak is constant under dynamic conditions. Second, we avoided the use of the quasi-equilibrium approximation (local chemical equilibrium between micelles and monomers). Third, we reduced the problem to a self-consistent system of four nonlinear differential equations. Its solution gives the concentration of surfactant monomers, total micelle concentration, mean aggregation number, and half-width of the micellar peak as functions of the spatial coordinates and time. Further, we checked the predictions of the model for the case of spatially uniform bulk perturbations (such as jumps in temperature, pressure or concentration). A detailed literature review could be found in [1].

Here, we apply the detailed model from [1] to investigate theoretically the problem about the kinetics of surfactant adsorption from micellar solutions. Many works have been dedicated to this subject [2–20]. The first theoretical model was developed by Lucassen [2] for the case of periodically expanding and contracting liquid surface. In this model, a complete local dynamic equilibrium between monomers and micelles has been assumed: the equilibrium mass-action law for the micelle reactions has been used. In such case, the surfactant transfer can be described as conventional diffusion-limited adsorption characterized by an apparent diffusion coefficient, D_A, which depends on the micellar concentration and aggregation number [11,12]. Because of the assumption for quasi-equilibrium between monomers and micelles, D_A is independent of the rate constants of the fast and slow micellization processes: k_{m}^{-} and k_{S}^{-}; for the definitions of the latter constants—see [1]. Correspondingly, if the quasi-equilibrium model by Lucassen [2] is applicable to a given experimental situation, then k_{m}^{-} and k_{S}^{-} cannot be determined from the obtained data for the dynamic surface tension or adsorption.

Later, Joos et al. [10–13] confirmed experimentally that in some cases the adsorption from micellar solutions could be described as diffusion-limited process characterized by an apparent diffusion coefficient, D_A, but the experimental data were not in agreement with the expression for D_A that follows from the Lucassen's model [2]. An alternative semiempirical expression for D_A was proposed [11,12], which agrees well with the experiment, but lacks a theoretical basis.

In subsequent studies, Joos et al. [14,15] established that sometimes the dynamics of adsorption from micellar solutions exhibits a completely different kinetic pattern: the interfacial relaxation is *exponential*, rather than *inverse-square-root*, as it is for the diffusion-limited kinetics. The theoretical developments [14,15,19] revealed that the exponential relaxation is influenced by the kinetics of the micellization processes, and from its analysis one could, in principle, determine the rate constants k_{m}^{-} and k_{S}^{-}. Thus, the physical picture becomes rather complicated. For example, for the surfactant Triton X-100 one obtains different types of adsorption kinetics depending on the used experimental method: exponential kinetics in the case of the inclined-plate method [14], and inverse-square-root kinetics for the maximum-bubble-pressure method [13].

Our main goal in the present paper is to give a general picture of the consecutive regimes of relaxation of the surface tension of a micellar surfactant solution. For this goal, we carried out a computer modeling of the adsorption process, based on the general system of equations derived in [1]. This analysis reveals the existence of four different consecutive regimes of interfacial relaxation for the same micellar surfactant solution: two exponential regimes and two inverse-square-root regimes, following one after another in alternating order. Experimentally, depending on the specific surfactant and method used, one typically registers one of these four regimes. Then, one has to identify which is the regime to interpret the obtained experimental results. To facilitate the data interpretation, we have derived convenient theoretical expressions for the time dependence of the surface tension and adsorption for each separate regime.

The paper is organized as follows. In Section 2, we give the general formulation of the problem for surfactant adsorption from micellar solution upon small perturbations, including the convective term in the mass-transport equations. In Section 3, we specify and simplify the basic set of differential equations and boundary conditions for the case of adsorption at a quiescent interface, after a small initial perturbation. The analysis of this case is the main subject of the present article. Numerical results for the relaxation of the surface tension, micelle concentration and aggregation number are presented in the form of kinetic diagrams, which reveal the stages of the relaxation process. In Section 4, in the case of regular kinetic diagram, we consider separately each of the four relaxation regimes and derive appropriate expressions describing theoretically the time dependence of the interfacial properties. Section 5 is devoted to the "rudimentary" kinetic diagrams, which could be observed at low micelle concentrations and/or at great

values of the rate constant of the fast micellization process. Merging or missing of some kinetic regimes characterizes such rudimentary diagrams.

The theoretical modeling of the dynamic surface tension of micellar surfactant solutions reported here reveals a general and physically rich picture of the adsorption process, which could find a direct application for the interpretation of experimental data.

2. General formulation of the problem for small perturbations

Let us first consider the general case of a planar fluid interface, which is subjected to uniform expansion and/or compression. Then, the interfacial area, A, becomes a function of time, t. We will assume that the initial surface area A_0 and the time dependence, $A=A(t)$, are known. The rate of surface dilatation, $\dot{\alpha}(t)$ and, the surface dilatation, $\dot{\alpha}(t)$, are defined as follows [21–24]:

$$\dot{\alpha}(t)\equiv\frac{1}{A}\frac{\mathrm{d}A}{\mathrm{d}t}=\frac{\mathrm{d}\alpha(t)}{\mathrm{d}t},\quad \alpha(t)=\int_0^t\dot{\alpha}\mathrm{d}t=\ln\frac{A(t)}{A_0} \tag{2.1}$$

One of the two neighboring fluid phases is assumed to be a micellar surfactant solution. The dilatation of the fluid interface gives rise to surfactant adsorption and diffusion. The diffusion flux leads to exchange of surfactant between the bulk and the interface. Both surfactant monomers and aggregates take part in the diffusion process. In addition, the aggregates (the micelles) exchange monomers between each other and with the surrounding solution (Fig. 1). As demonstrated in the first part of this study, this complex process can be adequately described by four functions of the position vector, $\boldsymbol{r}$, and time, t. These are the concentration of surfactant monomers, $c_1(\boldsymbol{r},t)$; the concentration of surfactant micelles, $C_\mathrm{m}(\boldsymbol{r},t)$; the mean aggregation number of the micelles, $m(\boldsymbol{r},t)$, and the half-width of the peak in the micellar size distribution (the polydispersity), $\sigma(\boldsymbol{r},t)$. A full system of nonlinear differential equations for determining the latter four functions has been derived in [1]. For small deviations from equilibrium (small perturbations), this system of equations can be linearized; see Eqs. (3.3)–(3.6) in [1]. Furthermore, substituting the expressions for the diffusion fluxes, Eqs. (2.22), (2.23) and (2.26), and reaction fluxes, Eqs. (3.7)–(3.9) in [1], the basic set of equation acquires the form:

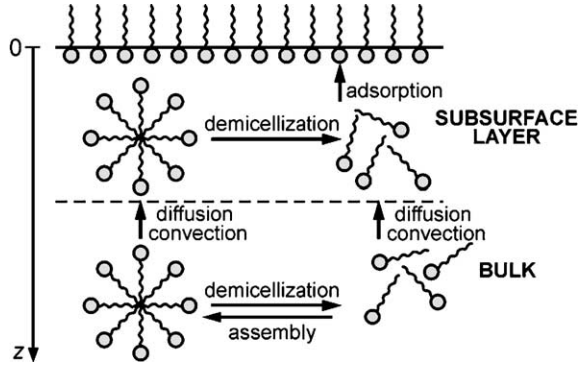

Fig. 1. Process of surfactant adsorption from micellar solutions. In the neighborhood of an expanded adsorption monolayer, the micelles release monomers to restore the equilibrium surfactant concentration at the surface and in the bulk. The concentration gradients give rise to bulk diffusion of both monomers and micelles.

$$\frac{\partial c_{1,\mathrm{p}}}{\partial t}-\dot{\alpha}z\frac{\partial c_{1,\mathrm{p}}}{\partial z}=\frac{D_\mathrm{o}}{S}\frac{\partial^2 c_{1,\mathrm{p}}}{\partial z^2}-k_\mathrm{S}^-\left(m_\mathrm{eq}-w\sigma_\mathrm{eq}\right)\times\frac{c_{1,\mathrm{eq}}}{S}f_\mathrm{s}-k_\mathrm{m}^-\frac{\beta c_{1,\mathrm{eq}}}{m_\mathrm{eq}S}f_\mathrm{m} \tag{2.2}$$

$$\frac{\partial C_{\mathrm{m,p}}}{\partial t}-\dot{\alpha}z\frac{\partial C_{\mathrm{m,p}}}{\partial z}=B_\mathrm{m}\frac{D_\mathrm{o}}{S}\frac{\partial^2 C_{\mathrm{m,p}}}{\partial z^2}+k_\mathrm{S}^-c_{1,\mathrm{eq}}f_\mathrm{s} \tag{2.3}$$

$$\frac{\partial m_\mathrm{p}}{\partial t}-\dot{\alpha}z\frac{\partial m_\mathrm{p}}{\partial z}=B_\mathrm{m}\frac{D_\mathrm{o}}{S}\frac{\partial^2 m_\mathrm{p}}{\partial z^2}-k_\mathrm{s}^-\frac{wm_\mathrm{eq}\sigma_\mathrm{eq}}{\beta}f_\mathrm{s}+k_\mathrm{m}^-f_\mathrm{m} \tag{2.4}$$

$$\frac{\partial\sigma_\mathrm{p}}{\partial t}-\dot{\alpha}z\frac{\partial\sigma_\mathrm{p}}{\partial z}=B_\mathrm{m}\frac{D_\mathrm{o}}{S}\frac{\partial^2\sigma_\mathrm{p}}{\partial z^2}+k_\mathrm{S}^-\left(w^2-1\right)\frac{\sigma_\mathrm{eq}m_\mathrm{eq}}{\beta}f_\mathrm{s}-\frac{k_\mathrm{m}^-}{2\sigma_\mathrm{eq}}f_\mathrm{m}-k_\mathrm{m}^-\frac{2}{\sigma_\mathrm{eq}^2}\sigma_\mathrm{p} \tag{2.5}$$

Here we use the same notations as in the first part of this study [1]. The subscripts "eq" and "p" mark the equilibrium values and the perturbations of the respective variables; z is the spatial coordinate along the normal to the interface (Fig. 1); k_m^- is the rate constant of monomer dissociation from the micelles; k_S^- is the rate constant of the slow micelle relaxation process, see Eq. (4.26) in [1]. S and D_o are defined as follows:

$$S\equiv\sum_{s=1}^{n_\mathrm{o}}s^2\frac{c_{s,\mathrm{eq}}}{c_{1,\mathrm{eq}}},\quad D_\mathrm{o}\equiv\sum_{s=1}^{n_\mathrm{o}}s^2\frac{c_{s,\mathrm{eq}}}{c_{1,\mathrm{eq}}}D_s \tag{2.6}$$

where the values of the summation index s correspond to the region of the surfactant monomers and oligomers, $s=1, 2, \ldots, n_\mathrm{o}$; $c_{s,\mathrm{eq}}$ and D_s are the equilibrium concentration and the diffusivity of the respective species; note that $S\geq 1$ and $D_\mathrm{o}\geq D_1$. A reasonable approximation is to assume that the concentrations of the oligomers, $c_{s,\mathrm{eq}}$ for $2\leq s\leq n_\mathrm{o}$, are negligible, and then $S=1$ and $D_\mathrm{o}=D_1$. In addition, we have introduced the notation:

$$B_\mathrm{m}\equiv SD_\mathrm{m}/D_\mathrm{o} \tag{2.7}$$

where D_m is the diffusivity of the micelles. The parameter β in Eqs. (2.2)–(2.5) is the equilibrium concentration of surfactant in micellar form, scaled by the critical micellization concentration, CMC:

$$\beta\equiv(C_\mathrm{tot}-\mathrm{CMC})/\mathrm{CMC}=m_\mathrm{eq}C_{\mathrm{m,eq}}/c_{1,\mathrm{eq}} \tag{2.8}$$

C_tot is the total surfactant concentration and $c_{1,\mathrm{eq}}=\mathrm{CMC}$. Another equilibrium dimensionless parameter is

$$w\equiv\left(m_\mathrm{eq}-n_\mathrm{r}\right)/\sigma_\mathrm{eq}>1 \tag{2.9}$$

where n_r is aggregation number at the boundary between the regions of the rare aggregates and the abundant micelles at equilibrium; σ_eq is the polydispersity of the equilibrium micelle

size distribution; see Fig. 1 in [1]. Finally, the quantities f_m and f_s are related to the reaction fluxes of the fast and slow micellization processes, $J_{m,0}$ and J, see [1]:

$$J_{m,0} = \frac{k_m^- \beta c_{1,eq}}{m_{eq}} f_m, \quad J = k_S^- c_{1,eq} f_s \tag{2.10}$$

$$f_m \equiv \frac{c_{1,p}}{c_{1,eq}} + \frac{\sigma_p - \sigma_{eq} m_p}{\sigma_{eq}^3} \tag{2.11}$$

$$f_s \equiv \left(m_{eq} - w\sigma_{eq}\right)\frac{c_{1,p}}{c_{1,eq}} - \frac{m_{eq} C_{m,p}}{\beta c_{1,eq}} + \frac{w m_p}{\sigma_{eq}} - \left(w^2 - 1\right)\frac{\sigma_p}{\sigma_{eq}} \tag{2.12}$$

In view of Eqs. (2.11) and (2.12), Eqs. (2.2)–(2.5) form a system of four linear differential equations for determining the evolution of the perturbations in the four basic parameters of the system: $c_{1,p}(z,t)$; $C_{m,p}(z,t)$; $m_p(z,t)$, and $\sigma_p(z,t)$. It should be noted also, that the convective terms in Eqs. (2.2)–(2.5), those containing $\dot{\alpha}$, are obtained by using the approximation of van Voorst Vader et al. [22], $\mathbf{v}\cdot\nabla c = -\dot{\alpha} z(\partial c/\partial z)$, where $\mathbf{v}$ is velocity and c is concentration; see also [18] and [25]. The validity of this approximation has been mathematically proven in [20,26,27]. This approximation is based on the fact that in most of the liquids, the thickness of the diffusion boundary layer is much smaller than the thickness of the hydrodynamic boundary layer.

To solve system (2.2)–(2.5) we need boundary conditions at the interface ($z=0$) and in the bulk of solution ($z\to\infty$). Based on the experimental results, it is usually accepted that the micelles do not adsorb at the interface, and that only the monomers can adsorb [4–20]. These assumptions lead to the following mass balance equations at the interface [1]:

$$\frac{\partial \Gamma_p}{\partial t} + \dot{\alpha}\Gamma_{eq} = D_o \frac{\partial c_{1,p}}{\partial z} \text{ at } z = 0 \text{ and } t > 0 \tag{2.13}$$

$$\frac{\partial C_{m,p}}{\partial z} = 0, \quad \frac{\partial m_p}{\partial z} = 0, \quad \frac{\partial \sigma_p}{\partial z} = 0 \text{ at } z = 0 \text{ and } t > 0 \tag{2.14}$$

Here Γ denotes surfactant adsorption; Γ_{eq} and $\Gamma_p = \Gamma - \Gamma_{eq}$ are its equilibrium value and perturbation. What concerns the other limit, $z\to\infty$, the perturbations $c_{1,p}(z,t)$; $C_{m,p}(z,t)$; $m_p(z,t)$, and $\sigma_p(z,t)$ are assumed to vanish in this limit (in the bulk of solution).

To close the set of boundary conditions, we have to specify the mechanism of surfactant adsorption. Here we will assume that the adsorption occurs under diffusion control. This is the most typical mechanism, although in some cases adsorption under barrier control could be also observed [15,19,28–34]. In the case of diffusion-limited adsorption, the subsurface layer of the solution is assumed to be in equilibrium with the adsorption layer at the interface. Then, the adsorption is related to the subsurface concentration of monomers by means of the equilibrium adsorption isotherm. For small perturbations, we have:

$$\Gamma_p = h_a c_{1,p}, \quad h_a \equiv \left(\frac{\partial \Gamma}{\partial c_1}\right)_{eq}, \quad \text{at } z = 0 \text{ and } t > 0 \tag{2.15}$$

Here h_a is the so-called adsorption length, which is to be calculated from the equilibrium surfactant adsorption isotherm, $\Gamma(c_1)$. For micellar solutions, h_a should be estimated at the critical micelle concentration, i.e., at $c_1 = \mathrm{CMC}$.

The general system of equations and boundary conditions described in the present section can be applied to describe the dynamics of surfactant adsorption under various dynamic regimes, corresponding to different experimental methods. For example, such regimes could correspond to quiescent, expanding, or oscillating interface. It turns out that the different dynamic regimes have different characteristic times, and correspond to different modified versions of the basis system of equations. For this reason, the different dynamic regimes demand separate treatment. In this paper, we will focus our attention on the detailed investigation of the relaxation of a quiescent interface after an initial small perturbation.

3. Adsorption at a quiescent interface after a small initial perturbation

The relaxation methods for measurement of dynamic surface tension [35–40] are based on an initial perturbation of the fluid interface, followed by diffusion of surfactant toward the immobile interface, and relaxation of the surfactant adsorption and the interfacial tension. At the initial moment, $t=0$, the deviation from equilibrium is characterized by the initial perturbation in adsorption, $\Gamma_p(0) = \Gamma(0) - \Gamma_{eq}$. For $t>0$, the interface is immobile, $\dot{\alpha}=0$ and, and the perturbation in adsorption, $\Gamma_p(t) = \Gamma(t) - \Gamma_{eq}$, tends to zero for $t\to\infty$. In the case of micellar surfactant solutions and small perturbations, this relaxation process is described by the system of Eqs. (2.2)–(2.5), and the boundary conditions, Eqs. (2.13)–(2.15), where we have to set $\dot{\alpha}=0$.

3.1. Dimensionless form of the basic equations

First, let us introduce the following dimensionless variables and constant parameters:

$$\zeta \equiv \frac{S}{h_a} z; \; \tau \equiv \frac{S D_o}{h_a^2} t; \quad K_s \equiv \frac{h_a^2}{S D_o} k_S^-; \quad K_m \equiv \frac{h_a^2}{S D_o} k_m^-. \tag{3.1}$$

Here, ζ, τ, K_s, and K_m are the dimensionless normal coordinate, z; time, t, and rate constants of the slow and fast micellar relaxation processes, k_S^- and k_m^-. Furthermore, it is convenient to scale the dependent variables as follows:

$$\xi_1 \equiv \frac{h_a}{\Gamma_p(0)} c_{1,p}; \; \xi_c \equiv \frac{h_a}{\beta \Gamma_p(0)} C_{m,p}; \; \xi_m \equiv \frac{h_a c_{1,eq}}{\sigma_{eq}^2 \Gamma_p(0)} m_p;$$

$$\xi_\sigma \equiv \frac{h_a c_{1,eq}}{\sigma_{eq} \Gamma_p(0)} \sigma_p \tag{3.2}$$

Here, ξ_1, ξ_c, ξ_m, and ξ_σ are the dimensionless *perturbations* in the concentration of surfactant monomers, $c_{1,p}$; micelle concentration, $C_{m,p}$; micelle mean aggregation number, m_p, and polydispersity of the abundant micelles, σ_p. It is important to note that the convenient definitions of the dimensionless perturbations ξ_1, ξ_c, ξ_m, and ξ_σ are different for different

dynamic problems. Here and in [1], we are using the same notation for the dimensionless perturbations of the same variables, despite some differences in the used scaling. This should not lead to any misunderstandings, because the treatment of different dynamic problems is completely independent here and in [1].

With the help of the above definitions, Eqs. (3.1) and (3.2), we bring the basic system of Eqs. (2.2)–(2.5), into the following dimensionless form:

$$\frac{\partial \xi_1}{\partial \tau} = \frac{\partial^2 \xi_1}{\partial \zeta^2} - \left(m_{\rm eq} - w\sigma_{\rm eq}\right)\frac{K_{\rm s}}{S}\varphi_{\rm s} - \frac{\beta K_{\rm m}}{m_{\rm eq} S}\varphi_{\rm m} \tag{3.3}$$

$$\frac{\partial \xi_c}{\partial \tau} = B_{\rm m}\frac{\partial^2 \xi_c}{\partial \zeta^2} + \frac{K_{\rm s}}{\beta}\varphi_{\rm s} \tag{3.4}$$

$$\frac{\partial \xi_m}{\partial \tau} = B_{\rm m}\frac{\partial^2 \xi_m}{\partial \zeta^2} - K_{\rm s}\frac{w m_{\rm eq}}{\beta\sigma_{\rm eq}}\varphi_{\rm s} + \frac{K_{\rm m}}{\sigma_{\rm eq}^2}\varphi_{\rm m} \tag{3.5}$$

$$\frac{\partial \xi_\sigma}{\partial \tau} = B_{\rm m}\frac{\partial^2 \xi_\sigma}{\partial \zeta^2} + K_{\rm s}\left(w^2-1\right)\frac{m_{\rm eq}}{2\beta}\varphi_{\rm s} - \frac{K_{\rm m}}{2\sigma_{\rm eq}^2}\varphi_{\rm m} - \frac{2K_{\rm m}}{\sigma_{\rm eq}^2}\xi_\sigma \tag{3.6}$$

Here, we have introduced the auxiliary notations.

$$\varphi_{\rm s} = \frac{h_{\rm a} c_{1,\rm eq}}{\Gamma_{\rm p}(0)} f_{\rm s}; \quad \varphi_{\rm m} = \frac{h_{\rm a} c_{1,\rm eq}}{\Gamma_{\rm p}(0)} f_{\rm m} \tag{3.7}$$

In terms of the new variables, defined by Eqs. (3.2) and (3.7), Eqs. (2.11) and (2.12) acquire the form:

$$\varphi_{\rm m} = \frac{h_{\rm a} m_{\rm eq}}{\Gamma_{\rm p}(0)\beta k_{\rm m}^-} J_{\rm m,0} = \xi_1 - \xi_m + \frac{\xi_\sigma}{\sigma_{\rm eq}^2} \tag{3.8}$$

$$\varphi_{\rm s} = \frac{h_{\rm a}}{\Gamma_{\rm p}(0) k_{\rm S}^-} J = \left(m_{\rm eq} - w\sigma_{\rm eq}\right)\xi_1 - m_{\rm eq}\xi_c + \sigma_{\rm eq} w \xi_m - \left(w^2-1\right)\xi_\sigma \tag{3.9}$$

Eq. (3.8) shows that if $\xi_\sigma \approx 0$ and $\xi_1 \approx \xi_m$, then $\varphi_{\rm m} \approx 0$, i.e., the system is equilibrated with respect to the *fast* micelle relaxation process, $J_{\rm m,0} \approx 0$. In addition, Eq. (3.9) implies that if $\xi_\sigma \approx 0$, and $\xi_1 \approx \xi_c \approx \xi_m$, then $\varphi_s \approx 0$, i.e., the system is equilibrated with respect to the *slow* micelle relaxation process, $J \approx 0$.

For small deviations from equilibrium, the relationships between interfacial tension, γ, and surfactant adsorption, Γ, as well as between Γ and the subsurface concentration of surfactant monomers, $c_1(0,t)$, are linear. Then, in view of Eq. (3.2), for the relative perturbations of these quantities we have:

$$\frac{\gamma(t) - \gamma_{\rm eq}}{\gamma(0) - \gamma_{\rm eq}} = \frac{\Gamma(t) - \Gamma_{\rm eq}}{\Gamma(0) - \Gamma_{\rm eq}} = \xi_1(0,\tau) \equiv \xi_{1,0}(\tau) \tag{3.10}$$

see also Eqs. (2.15) and (3.2); $\xi_{1,0}(\tau)$ is the dimensionless perturbation of the subsurface concentration of surfactant monomers as a function of the dimensionless time, τ.

With the help of Eqs. (3.1) (3.2) and (3.10), setting $\dot{\alpha} = 0$ and we obtain the dimensionless form of the boundary conditions, Eqs. (2.13) and (2.14):

$$\frac{\partial \xi_1}{\partial \tau} = \frac{\partial \xi_1}{\partial \zeta}; \quad \frac{\partial \xi_c}{\partial \zeta} = \frac{\partial \xi_m}{\partial \zeta} = \frac{\partial \xi_\sigma}{\partial \zeta} = 0, \quad \text{at } \zeta = 0 \text{ and } \tau > 0. \tag{3.11}$$

In the bulk of solution ($\zeta \to \infty$), all perturbations vanish. In addition, the initial conditions (at $t = 0$) are:

$$\xi_1(0,0) = 1; \quad \xi_1(\zeta,0) = 0 \text{ for } \zeta > 0 \tag{3.12}$$

$$\xi_c(\zeta,0) = \xi_m(\zeta,0) = \xi_\sigma(\zeta,0) = 0 \text{ for } \zeta \geq 0 \tag{3.13}$$

The system of differential equations, Eqs. (3.3)–(3.6), together with the boundary conditions, Eq. (3.11), and the initial conditions, Eqs. (3.12) and (3.13) can be solved numerically, as described in Appendix A. The results are reported below.

3.2. Parameters of the micellar system

To investigate the relaxation of adsorption and surface tension of micellar surfactant solutions, we calculated numerically the time evolution of the subsurface values (at $z = 0$) of the parameters of the micellar solution: $\xi_{1,0}(\tau) \equiv \xi_1(0,\tau)$; $\xi_{c,0}(\tau) \equiv \xi_c(0,\tau)$; $\xi_{m,0}(\tau) \equiv \xi_m(0,\tau)$, and $\xi_{\sigma,0}(\tau) \equiv \xi_\sigma(0,\tau)$, see Fig. 2. In our computations, we assigned typical values to the following constant parameters of the system:

$$S = 1.1,\ m_{\rm eq} = 60,\ \sigma_{\rm eq} = 5,\ w = 3,\ K_{\rm m} = 10^3,\ B_{\rm m} = 0.2 \tag{3.14}$$

The rate constant of the slow process, $K_{\rm s}$, is varied. To illustrate its influence, we obtained numerical data for the following three values: $K_{\rm m}/K_{\rm s} = 10^5$ (Fig. 2a); $K_{\rm m}/K_{\rm s} = 10^6$ (Fig. 2b), and $K_{\rm m}/K_{\rm s} = 10^7$ (Fig. 2c).

In [1], we developed a general procedure for determination of the three micellar relaxation times as roots of a cubic characteristic equation; see Eq. (4.30) in [1]. Two of them, t_m and t_σ, characterize the fast relaxation process, while the third one, t_c, characterizes the slow relaxation process. In general, t_c, t_m and t_σ are related to the relaxation of the three independent perturbations: in the micelle concentration, ξ_c; in the micelle mean aggregation number, ξ_m, and in the micelle polydispersity, ξ_σ, respectively. At low micelle concentrations we have $t_c > t_m > t_\sigma$, while at high micelle concentrations the two fast relaxation times exchange their positions: $t_c > t_\sigma > t_{\rm m}$; see [1] for details.

In our computations, we obtain the dimensionless micellar relaxation times (for details—see below):

$$\tau_i = k_{\rm m}^- t_i = K_{\rm m}\theta_i \quad (i = c, m, \sigma) \tag{3.15}$$

Here τ_i, and $\theta_i = \tau_i/K_{\rm m}$ are the dimensionless relaxation times corresponding to the scaling used, respectively, in [1] and here, see Eq. (3.1). Values of θ_c, θ_m, and θ_σ, corresponding to different $K_{\rm m}/K_{\rm s}$ and micelle concentration $\beta \equiv (C_{\rm tot} - {\rm CMC})/{\rm CMC}$, are listed in Table 1. To compute the values in Table 1,

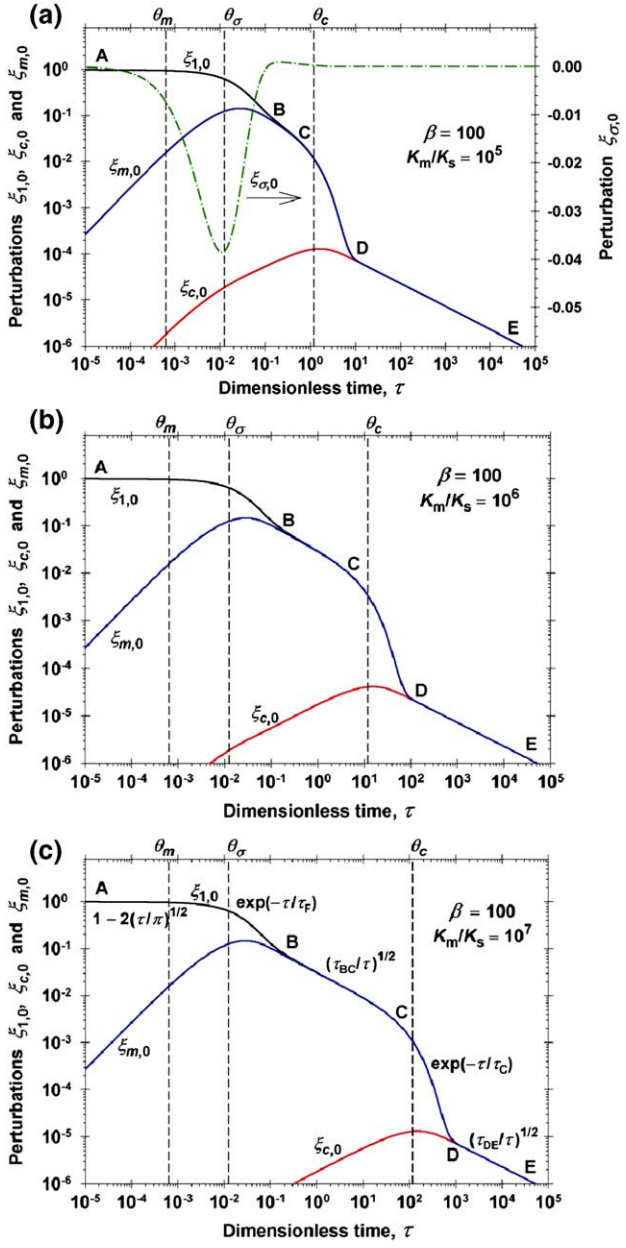

Fig. 2. Time dependence of the perturbations in the subsurface (at $z=0$) monomer concentration, $\xi_{1,0}$, micelle concentration, $\xi_{c,0}$, mean aggregation number, $\xi_{m,0}$, and polydispersity, $\xi_{\sigma,0}$, for $\beta=100$; the other parameters are given by Eq. (3.14). $\xi_{1,0}$ expresses also the dimensionless perturbation in surface tension and adsorption, see Eq. (3.10). The curves are obtained by numerical solution of the general system of equations in Section 3.1. (a) $K_m/K_s=10^5$; (b) $K_m/K_s=10^6$; (c) $K_m/K_s=10^7$. $\xi_{\sigma,0}$, which is similar for (a), (b) and (c), is shown only in (a). In (c) it is illustrated that the relaxation of $\xi_{1,0}$ exhibits two exponential regimes (AB and CD), and two inverse-square-root regimes (BC and DE), with different characteristic times, τ_F, τ_C, τ_{BC}, and τ_{DE} (see the text). θ_m, θ_σ and θ_c are the three characteristic micellization times (Table 1).

we first calculated τ_c, τ_m, and τ_σ using the procedure developed in [1]. The respective values of θ_c, θ_m, and θ_σ are shown by vertical dashed lines in Fig. 2 to show how they are related to the stages of the interfacial relaxation. Table 1 indicates that θ_c is sensitive to the variation of both β and K_m/K_s;θ_m is sensitive to β, but insensitive to K_m/K_s; θ_σ is insensitive to both β and K_m/K_s.

3.3. Numerical results and discussion

The results reported here are obtained by solving numerically the general system of equations in Section 3.1 by means of the numerical procedure described in Appendix A. The calculated curves $\xi_{1,0}(\tau)$, $\xi_{c,0}(\tau)$, and $\xi_{m,0}(\tau)$ are shown in Fig. 2 for a relatively high micelle concentration, $\beta=100$. The perturbation $\xi_{\sigma,0}(\tau)$, which is similar for Fig. 2a, b and c, is shown only in Fig. 2a. Note that $\xi_{1,0}$ expresses not only the perturbation in the subsurface monomer concentration, but also the perturbations in the surface tension and adsorption, see Eq. (3.10).

The general picture in a regular kinetic diagram (Fig. 2) is the following. At the initial stage (denoted by A) the perturbation of the subsurface concentration of monomers is $\xi_{1,0}\approx1$, while the other perturbations, $\xi_{c,0}$, $\xi_{m,0}$, and $\xi_{\sigma,0}$, are ≈0. In the limit of long times, $\tau\to\infty$, all perturbations become zero again. For this reason, $\xi_{c,0}$, $\xi_{m,0}$, and $\xi_{\sigma,0}$ have extremum, while $\xi_{1,0}$ monotonically decays with time. Note, that the minimum of $\xi_{\sigma,0}$ and the maximum of $\xi_{c,0}$ correspond to the respective micellar relaxation times, θ_σ and θ_c. In contrast, the maximum of $\xi_{m,0}(\tau)$ appears at $\tau\neq\theta_m$.

The most important feature of the relaxation curves (Fig. 2) is that $\xi_{m,0}$ merges with $\xi_{1,0}$ at a given point, denoted by B, while $\xi_{c,0}$ merges with $\xi_{1,0}$ (and $\xi_{m,0}$) at another point, denoted by D. The moments of time, corresponding to the points B and D, will be denoted below by τ_B and τ_D, respectively. As seen in Fig. 2, for $\tau>\tau_B$, we have $\xi_{\sigma,0}\approx0$ and $\xi_{1,0}=\xi_{m,0}$. In view of Eq. (3.8), this means that for $\tau>\tau_B$ the flux of the fast micelle relaxation process, $J_{m,0}$, is equal to zero. In other words, for $\tau>\tau_B$ the monomers and micelles are equilibrated with respect to the *fast* relaxation process. It turns out that for a regular relaxation process $\tau_B\approx2\theta_\sigma^{1/2}$, see Eq. (4.9).

In Section 4 we derive asymptotic analytical expressions describing the regions AB, BC, CD and DE of the relaxation curve $\xi_{1,0}(\tau)$ (Fig. 2). In particular, the point C corresponds to the moment $\tau_C\approx\theta_c$. It turns out that $\xi_{1,0}(\tau)$ exhibits two exponential regimes, AB and CD, and two inverse-square-root regimes, BC and DE, see Fig. 2b. Expressions for the respective characteristic adsorption relaxation times, τ_F, τ_C, τ_{BC}, and τ_{DE}, are also derived.

It should be also noted that in addition to the regular kinetic diagrams (Fig. 2 and Section 4) one could sometimes observe a "rudimentary" kinetic diagram, characterized by merging or disappearance of the stages BC and CD, see Section 5.

Table 1
Calculated values of the dimensionless micellar relaxation times, θ_c, θ_m, and θ_σ

Relax. time	$K_m/K_s=10^5$	$K_m/K_s=10^6$	$K_m/K_s=10^7$
$\beta=1$			
θ_c	5.44×10^{-2}	4.21×10^{-1}	4.12×10^{0}
θ_m	1.82×10^{-2}	1.86×10^{-2}	1.87×10^{-2}
θ_σ	9.41×10^{-3}	1.19×10^{-2}	1.21×10^{-2}
$\beta=100$			
θ_c	1.20×10^{0}	1.18×10^{1}	1.18×10^{2}
θ_m	6.36×10^{-4}	6.42×10^{-4}	6.43×10^{-4}
θ_σ	1.25×10^{-2}	1.25×10^{-2}	1.25×10^{-2}

4. Stages of a regular kinetic diagram

4.1. Initial relaxation regime AB

For the initial relaxation regime (stage) AB (Fig. 2), we have $\xi_{c,0} \approx \xi_{m,0} \approx \xi_{\sigma,0} \approx 0$. Hence, the respective terms in Eqs. (3.3) (3.8) and (3.9) can be neglected. Thus, Eq. (3.3) acquires the form:

$$\frac{\partial \xi_1}{\partial \tau} = \frac{\partial^2 \xi_1}{\partial \zeta^2} - (1+R_s)^2 \frac{\beta K_m}{m_{eq} S} \xi_1 \tag{4.1}$$

where the parameter R_s characterizes the relative importance of the slow micellar process with respect to the fast one:

$$R_s \equiv m_{eq}\left(m_{eq} - w\sigma_{eq}\right)^2 \frac{K_s}{\beta K_m} \tag{4.2}$$

For the parameter values in Eq. (3.14), we obtain:

$$R_s = 1.215 \times 10^5 \frac{K_s}{\beta K_m} \tag{4.3}$$

Thus, for $K_m/K_s \geq 10^5$ and $\beta = 100$ (Fig. 2), Eq. (4.3) yields $R_s \ll 1$, and the contribution of the slow process is negligible; then R_s could be neglected in Eq. (4.1). In contrast, for $K_m/K_s = 10^5$ and $\beta = 1$ (low micelle concentration, see Section 5), Eq. (4.3) yields $R_s \approx 1$, and the contribution of the slow process becomes considerable.

Eq. (4.1) represents a diffusion equation with a linear reaction (source) term. Similar equation was first used in the theory of adsorption from micellar solutions by Rillaerts and Joos [41], and subsequently applied by many other authors [9,15,17,19,30,42,43]. The novel information in our Eq. (4.1) is that the coefficient before ξ_1 in the reaction term is obtained in explicit form. One sees that this coefficient is related to the micellar concentration and mean aggregation number, β and m_{eq}; to the width of the micellar peak, w, and to the dimensionless rate constants of the fast and slow micellar processes, K_m and K_s.

From a kinetic viewpoint, every chemical reaction, irrespective of its order, yields a linear reaction term in the case of *small deviations* from equilibrium, when the respective term can be linearized. This approximation is known as pseudo-first-order-reaction (PFOR) model, which is widely used in chemical kinetics; see e.g., [44]. Mathematically, Eq. (4.1) is a linear differential equation for ξ_1. The Laplace transform of ξ_1 can be easily found, but it is a nontrivial task to find the original ξ_1 in explicit analytical form. As we are interested in dynamic surface tension and adsorption, see Eq. (3.10), we will use the exact solution for $\xi_{1,0}(\tau)$ obtained in [19] in a closed form:

$$\xi_{1,0}(\tau) = \frac{s_F - 1}{s_F} \exp\left(-\frac{s_F - 1}{2}\tau\right) + \frac{2}{\pi}\int_0^\infty \exp\left[-\left(\frac{1}{\tau_F} + \tilde{\tau}^2\right)\tau\right] \frac{\tilde{\tau}^2}{\left(\tilde{\tau}^2 + 1/\tau_F\right)^2 + \tilde{\tau}^2} d\tilde{\tau} \tag{4.4}$$

To derive Eq. (4.4), the initial condition, Eq. (3.12), and the boundary condition for $\xi_1(\zeta \to \infty) = 0$ have been used. Eq. (4.4) is applicable only for the regime AB; $\tilde{\tau}$ is an integration variable; the characteristic relaxation time, τ_F, and the parameter, s_F, are defined by the expressions:

$$\frac{1}{(1+R_s)\tau_F} \equiv \frac{\beta K_m}{m_{eq} S} \approx \frac{1}{\theta_m} - \frac{1}{2\theta_\sigma}, \quad s_F \equiv \left(1 + \frac{4}{\tau_F}\right)^{1/2} \tag{4.5}$$

To obtain the relationship between τ_F and the two fast micellar relaxation times, θ_m and θ_σ, we used Eq. (4.45) in [1]. At sufficiently high micelle concentrations, we have $\theta_m \ll \theta_\sigma$ and $R_s \ll 1$; then $\tau_F \approx \theta_m$.

For *short* times, $\tau \ll 1$, Eq. (4.4) has a simple asymptotics, which coincides with the respective asymptotics for diffusion-controlled adsorption, see [19] and [45]:

$$\xi_{1,0} = 1 - 2\left(\frac{\tau}{\pi}\right)^{1/2} + \tau + \cdots \quad (\text{short} - \text{time asymptotics}) \tag{4.6}$$

Eq. (4.6) implies that the time limiting factor at short times is the diffusion of surfactant monomers; see the definition of τ in Eq. (3.1).

The *long*-time (for $\tau \to \infty$) asymptotics of Eq. (4.4) is [19]:

$$\xi_{1,0} = \frac{s_F - 1}{s_F} \exp\left(-\frac{s_F - 1}{2}\tau\right) + \cdots \quad (\text{long} - \text{time asymptotics}) \tag{4.7}$$

where the higher order terms are neglected. In particular, for $4/\tau_F \ll 1$, we have $(s_F - 1)/2 \approx 1/\tau_F$. Then, Eq. (4.7) reduces to:

$$\xi_{1,0} \approx \frac{2}{\tau_F} \exp\left(-\frac{\tau}{\tau_F}\right) + \cdots \quad \left(\text{for } \frac{4}{\tau_F} \ll 1\right) \tag{4.8}$$

Thus, in contrast with the short-time limit, Eq. (4.6), the long-time limit, Eqs. (4.7) and (4.8), is affected by the presence of micelles through τ_F, which is related to the characteristic times of the fast micellar process, θ_m and θ_σ, see Eq. (4.5). Moreover, Eqs. (4.7) and (4.8) predict exponential decay of the perturbation $\xi_{1,0}(\tau)$, instead of the much slower, inverse-square-root decay for concentrations below the CMC [45]. Such an exponential decay has been experimentally detected for micellar solutions of Triton X-100 by means of the inclined-plate method, see [14] and [19]. From the fits of experimental data, one can determine τ_F and then from the slope of the plot $1/\tau_F$ vs. β, one could obtain the rate constant of the fast process, K_m; see Eq. (4.5) and [19].

It is important to note that the simplified model, based on Eq. (4.1), and its solution, Eq. (4.4), is valid only during the stage AB (Fig. 2). After the point B (for $\tau > \tau_B$), where the fast micellar process attains equilibrium, the dependence $\xi_{1,0}(\tau)$ could not be dependent on the kinetic parameter τ_F. It turns out that for $\tau > \tau_B$, the exponential decay is transformed into inverse-square-root decay; see Section 4.3. In other words, Eqs. (4.4), (4.7) and (4.8) could be applied only for $\tau < \tau_B$.

Analyzing the Laplace transforms of Eqs. (3.5) and (3.6), along with Eq. (3.8), and comparing the different time-scales

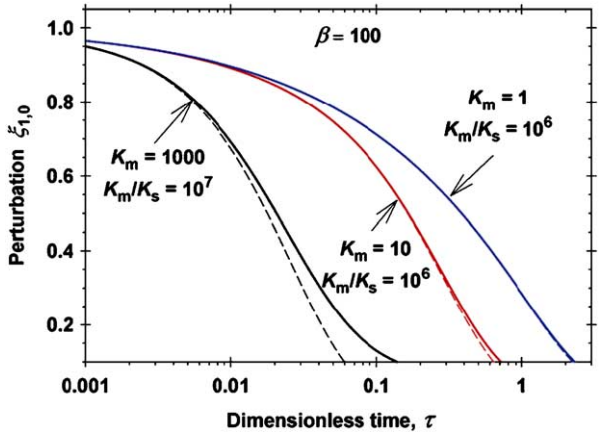

Fig. 3. Comparison of the approximate analytical solution, Eq. (4.4), the dashed lines, with the exact numerical solution of the system in Section 3.1, the solid lines. The values of K_m and K_m/K_s are denoted in the figure; the other parameters are given by Eq. (3.14).

with the numerical results for τ_B, we arrived at the following semi-empirical expression:

$$\tau_B = \left(\frac{2\sigma_{eq}^2}{K_m}\right)^{1/2} = 2\theta_\sigma^{1/2} \tag{4.9}$$

See Eq. (4.45) in [1] for θ_σ. The above expression is related to the factor $K_m/(2\sigma_{eq}^2)$ that appears before φ_m in Eqs. (3.5) and (3.6).

In Fig. 3, the integral asymptotic solution, Eq. (4.4), the dashed curves, is checked against the exact solution of the general system of equations in Section 3.1 (the full curves). One sees that for the lower values of K_m (1 and 10) there is an excellent agreement between the two types of curves. On the other hand, for $K_m=1000$ the agreement is not so good. In such cases, the exact numerical solution (Section 3.1) should be used. On the other hand, in Fig. 3 the exact and asymptotic curves merge for small τ. Hence, the short-time asymptotics, Eq. (4.6), has a greater range of validity with respect to the values of the rate constants K_m and K_s.

4.2. Equilibrated fast micellar process: region BCDE

As mentioned above, for $\tau>\tau_B$ we have $\xi_{\sigma,0}\approx 0$ and $\xi_{1,0}=\xi_{m,0}$, and consequently, the reaction flux of the fast micellar process is $J_{m,0}=0$, see Eq. (3.8) and Fig. 2. In other words, micelles and monomers are equilibrated with respect to the fast process along the whole region BCDE (Fig. 2). From the viewpoint of the theoretical description, $\xi_{\sigma,0}\approx 0$ means that in the general system of equations we could skip Eq. (3.6). Furthermore, $\xi_{1,0}=\xi_{m,0}$ implies that Eqs. (3.3) and (3.5) could be combined into a single mass balance equation. To eliminate the terms with φ_m, we multiply Eq. (3.5) by $\beta\sigma_{eq}^2/(m_{eq}S)$ and sum the result with Eq. (3.3):

$$\frac{\partial}{\partial\tau}\left(\xi_1+\frac{\beta\sigma_{eq}^2}{m_{eq}S}\xi_m\right)=\frac{\partial^2}{\partial\zeta^2}\left(\xi_1+\frac{\beta\sigma_{eq}^2}{m_{eq}S}B_m\xi_m\right)-m_{eq}\frac{K_s}{S}\varphi_s \tag{4.10}$$

The boundary condition for Eq. (4.10) requires a special derivation. For this goal, let us consider a small cylinder of height, L, and bases parallel to the interface. Integrating Eq. (4.10) for $0\le\zeta\le L$, along with the boundary conditions $\partial\xi_1/\partial\zeta=\partial\xi_1/\partial\tau$ and $\partial\xi_m/\zeta=0$ at $\zeta=0$ (see Eq. (3.11)), yields:

$$\int_0^L\left[\frac{\partial}{\partial\tau}\left(\xi_1+\frac{\beta\sigma_{eq}^2}{m_{eq}S}\xi_m\right)+m_{eq}\frac{K_s}{S}\varphi_s\right]d\zeta$$
$$=\frac{\partial}{\partial\zeta}\left(\xi_1+\frac{\beta\sigma_{eq}^2}{m_{eq}S}B_m\xi_m\right)\Big|_{\zeta=L}-\frac{\partial\xi_1}{\partial\tau}\Big|_{\zeta=0} \tag{4.11}$$

Next, in Eq. (4.11) we make the transition $L\to 0$ and use the relationship $\xi_m\approx\xi_1$, which is fulfilled in the region BCDE (Fig. 2). Thus, we obtain the boundary condition in the form:

$$\frac{\partial\xi_1}{\partial\tau}=\left(1+\frac{\beta\sigma_{eq}^2}{m_{eq}S}B_m\right)\frac{\partial\xi_1}{\partial\zeta}\quad\text{at }\zeta=0\text{ and }\tau>\tau_B \tag{4.12}$$

Furthermore, using again the relationships $\xi_{\sigma,0}=0$ and $\xi_{1,0}=\xi_{m,0}$, along with Eq. (3.9), we bring the mass-transport Eqs. (4.10) and (3.4) into the form:

$$\left(1+\frac{\beta\sigma_{eq}^2}{m_{eq}S}\right)\frac{\partial\xi_1}{\partial\tau}=\left(1+\frac{\beta\sigma_{eq}^2}{m_{eq}S}B_m\right)\frac{\partial^2\xi_1}{\partial\zeta^2}-\frac{m_{eq}^2K_s}{S}(\xi_1-\xi_c) \tag{4.13}$$

$$\frac{\partial\xi_c}{\partial\tau}=B_m\frac{\partial^2\xi_c}{\partial\zeta^2}+\frac{m_{eq}K_s}{\beta}(\xi_1-\xi_c) \tag{4.14}$$

Thus, we replace the general system, Eqs. (3.3)–(3.6) and the boundary condition Eq. (3.11), with a simplified boundary problem consisting of Eqs. (4.12)–(4.14). In [9], the model based on the latter simplified system is called “diffusion affected by the slow relaxation process”; see Eqs. (3.15a) and (3.15b) in [9]. Note, however, that the correct boundary condition for the simplified system is Eq. (4.12), rather than $\partial\xi_1/\partial\zeta=\partial\xi_1/\partial\tau$, which has been used in [9]. Joos et al. [11,12], were the first who derived the correct boundary condition for the case of monodisperse micelles, which is analogous to Eq. (4.12). Finally, we recall that the simplified model, based on Eqs. (4.12)–(4.14), is applicable only for $\tau>\tau_B$ (equilibrated fast micellar process).

4.3. Relaxation regime BC

The relaxation regime BC (Fig. 2), that occurs at $\tau_B<\tau<\tau_C$, is a sub-domain of the greater region BCDE considered in the previous subsection. Here, τ_C can be identified with the characteristic time of the slow micellar relaxation process:

$$\tau_C\equiv\theta_c\approx\frac{\beta\sigma_{eq}^2}{m_{eq}^3K_s} \tag{4.15}$$

At the last step we have used Eq. (4.43) in [1] for $\beta>>1$ and $m_{eq}^2>>\sigma_{eq}^2$. For $\tau<\tau_C$, the slow micellar process has not yet been activated. For this reason, in the region BC we have $\xi_c<<1$, and the reaction flux due to the slow process gives a

negligible contribution in the mass balance of surfactant. Then, we could skip Eq. (4.14) and neglect the last term in Eq. (4.13), which acquires the form:

$$\left(1+\frac{\beta\sigma_{\rm eq}^2}{m_{\rm eq}S}\right)\frac{\partial\xi_1}{\partial\tau}=\left(1+\frac{\beta\sigma_{\rm eq}^2}{m_{\rm eq}S}B_{\rm m}\right)\frac{\partial^2\xi_1}{\partial\zeta^2} \tag{4.16}$$

Eq. (4.16) has to be solved in combination with the boundary condition, Eq. (4.12). This mathematical problem is analogous to the known kinetic problem for diffusion-limited adsorption below the CMC [45]. In view of the initial condition, Eq. (3.12), the solution of this problem reads:

$$\xi_{1,0}(\tau)=\exp(\tau/\tau_{\rm BC})\mathrm{erfc}\left((\tau/\tau_{\rm BC})^{1/2}\right) \tag{4.17}$$

where $\mathrm{erfc}(x)$ is the complementary error function [46], and

$$\frac{1}{\tau_{\rm BC}}=\left(1+\frac{\beta\sigma_{\rm eq}^2}{m_{\rm eq}S}\right)\left(1+\frac{\beta\sigma_{\rm eq}^2}{m_{\rm eq}S}B_{\rm m}\right) \tag{4.18}$$

Because in the region BC we have $\tau/\tau_{\rm BC}>\tau_{\rm B}/\tau_{\rm BC}\gg1$, we have to use only the asymptotic form of Eq. (4.17), viz.

$$\xi_{1,0}(\tau)\approx\left(\frac{\tau_{\rm BC}}{\pi\tau}\right)^{1/2}\quad(\tau_{\rm B}<\tau<\tau_{\rm C}) \tag{4.19}$$

In other words, in the region BC the relaxation process is described as diffusion controlled, with an inverse-square-root dependence of time, Eq (4.19). Note that the characteristic time, $\tau_{\rm BC}$, Eq. (4.18), depends on the diffusion coefficients and the equilibrium parameters, but it is independent of the rate constants of the fast and slow micellar processes, $K_{\rm m}$ and $K_{\rm s}$.

In the case of diffusion-controlled adsorption below the CMC, the characteristic relaxation time is $t_r=h_{\rm a}^2/D$, where D is diffusivity. In analogy with the latter relationship, for the micellar solution one could define an *apparent surfactant diffusivity* for the region BC: $D_{\rm BC}\equiv h_{\rm a}^2/t_{\rm BC}=SD_{\rm o}/\tau_{\rm BC}$, where $t_{\rm BC}$ is the dimensional time, corresponding to $\tau_{\rm BC}$; see Eq. (3.1). Thus, the multiplication of Eq. (4.18) by $SD_{\rm o}$ yields:

$$D_{\rm BC}=SD_o\left(1+\frac{\beta\sigma_{\rm eq}^2}{m_{\rm eq}S}\right)\left(1+\frac{\beta\sigma_{\rm eq}^2}{m_{\rm eq}S}B_{\rm m}\right) \tag{4.20}$$

If we set $m_{\rm eq}S/\sigma_{\rm eq}^2\approx1$, Eq. (4.20) reduces to the semi-empirical expression for the effective diffusivity in a micellar solution, obtained by Joos et al. [11,12]. Indeed, for typical parameter values, $m_{\rm eq}=60$, $\sigma_{\rm eq}=8$, and $S=1.1$, we really get $m_{\rm eq}S/\sigma_{\rm eq}^2\approx1$.

Experimentally, an inverse-square-root dependence of time, Eq. (4.19), has been observed in a number of studies on kinetics of adsorption from *micellar* surfactant solutions. Such dependence has been established for the nonionic surfactant Brij 58 by means of the dynamic drop-volume method [10,11], and by means of the stripe method [12]. Analogous results have been obtained for the surfactant Triton X-100 by means of the maximum-bubble-pressure method [13]. In particular, a good agreement between experiment and theory (Eq. (4.20) with $m_{\rm eq}S/\sigma_{\rm eq}^2\approx1$) was reported in [12]. Our analysis indicates that the adsorption kinetics detected in these experiments corresponds to the kinetic regime BC (Fig. 2).

4.4. Relaxation regime DE

The theoretical analysis of the relaxation regime DE is analogous to that of BC. (The intermediate region CD is considered in Section 4.5 below.) After the point D, i.e., for $\tau>\tau_{\rm D}$, we have $\xi_{c,0}=\xi_{m,0}=\xi_{1,0}$, and $\xi_{\sigma,0}\approx0$ (Fig. 2). The substitution of the latter relationships into Eqs. (3.8) and (3.9) leads to the conclusion that the reaction fluxes of both the fast and slow micellar processes are equal to zero: $\varphi_{\rm m}=\varphi_{\rm s}=0$ for $\tau>\tau_{\rm D}$. In other words, the micelles are completely equilibrated with the monomers. In such a case, Eqs. (3.3)–(3.5) can be combined into a single mass balance equation for the surfactant. For this goal, we multiply Eq. (3.4) by $m_{\rm eq}\beta/S$, and sum it with Eq. (4.10). The result reads:

$$\frac{\partial}{\partial\tau}\left(\xi_1+\frac{\beta\sigma_{\rm eq}^2}{m_{\rm eq}S}\xi_m+\frac{m_{\rm eq}\beta}{S}\xi_c\right)=\frac{\partial^2}{\partial\zeta^2}\left(\xi_1+\frac{\beta\sigma_{\rm eq}^2}{m_{\rm eq}S}B_{\rm m}\xi_m+\frac{m_{\rm eq}\beta}{S}B_{\rm m}\xi_c\right) \tag{4.21}$$

Following the derivation of Eq. (4.12), we integrate Eq. (4.21) to deduce the boundary condition

$$\frac{\partial\xi_1}{\partial\tau}=\left(1+B_m\frac{\sigma_{\rm eq}^2+m_{\rm eq}^2}{m_{\rm eq}S}\beta\right)\frac{\partial\xi_1}{\partial\zeta}\ \text{at}\ \zeta=0\ \text{and}\ \tau>0 \tag{4.22}$$

Furthermore, in Eq. (4.21) we substitute $\xi_{c,0}=\xi_{m,0}=\xi_{1,0}$, and obtain the combined mass balance equation for the surfactant in the kinetic region DE:

$$\left(1+\beta\frac{\sigma_{\rm eq}^2+m_{\rm eq}^2}{m_{\rm eq}S}\right)\frac{\partial\xi_1}{\partial\tau}=\left(1+\beta\frac{\sigma_{\rm eq}^2+m_{\rm eq}^2}{m_{\rm eq}S}B_{\rm m}\right)\frac{\partial^2\xi_1}{\partial\zeta^2} \tag{4.23}$$

Eq. (4.23) has to be solved in combination with the boundary condition, Eq. (4.22). Again, this mathematical problem is similar to the known kinetic problem for diffusion-limited adsorption below the CMC [45]. In the same way, as in Section 4.3, we derive analogues of Eqs. (4.18) (4.19) and (4.21):

$$\frac{1}{\tau_{\rm DE}}\equiv\left(1+\beta\frac{\sigma_{\rm eq}^2+m_{\rm eq}^2}{m_{\rm eq}S}\right)\left(1+\beta\frac{\sigma_{\rm eq}^2+m_{\rm eq}^2}{m_{\rm eq}S}B_{\rm m}\right) \tag{4.24}$$

$$\xi_{1,0}(\tau)\approx\left(\frac{\tau_{\rm DE}}{\pi\tau}\right)^{1/2}\quad(\tau>\tau_{\rm D}) \tag{4.25}$$

$$D_{\rm DE}=SD_{\rm o}\left(1+\beta\frac{\sigma_{\rm eq}^2+m_{\rm eq}^2}{m_{\rm eq}S}\right)\left(1+\beta\frac{\sigma_{\rm eq}^2+m_{\rm eq}^2}{m_{\rm eq}S}B_{\rm m}\right) \tag{4.26}$$

Thus, in the region DE the relaxation process is described as diffusion controlled, with an inverse-square-root dependence of

time, Eq. (4.25). Note that the characteristic time, τ_{DE}, depends on the diffusion coefficients and the equilibrium parameters, but it is independent of the rate constants of the fast and slow micellar processes, K_m and K_s; see Eq. (4.24).

For micellar systems we typically have $S \approx 1$, $D_o \approx D_1$, and $m_{eq}^2 >> \sigma_{eq}^2$. Then, Eq. (4.26) reduces to:

$$D_{DE} \approx D_1 \left(1 + \beta m_{eq}\right)\left(1 + \beta m_{eq} B_m\right) \tag{4.27}$$

An expression analogous to Eq. (4.27) has been derived by Lucassen [2] for a model assuming monodisperse micelles of aggregation number m_{eq}. He found a good agreement of this model with experimental data for adsorption of the nonionic surfactants $C_{12}E_6$ and $C_{14}E_6$ at a liquid interface that is subjected to small sinusoidal compression and expansion [2,3].

Because $m_{eq}^2 >> \sigma_{eq}^2$, the dependence $D_{DE}(\beta)$, predicted by Eq. (4.26) is much stronger than the dependence $D_{BC}(\beta)$, predicted by Eq. (4.20). Of course, the same is true for the dependencies $\tau_{DE}(\beta)$ and $\tau_{BC}(\beta)$, given by Eqs. (4.24) and (4.18). The latter fact enables one to easily distinguish between the regimes BC and DE (both of them corresponding to inverse-square-root time dependence), when interpreting a set of experimental data for the dependence of the apparent diffusivity (or relaxation time) on β. For example, Joos et al. [10–12] established a considerable disagreement between their experimental data and the Lucassen's Eq. (4.27). The reason is that the data by Joos et al. correspond to the regime BC, while the Lucassen's Eq. (4.27) is derived for the regime DE (the two regimes have not been distinguished at that time).

4.5. Compound asymptotic expression for the region BCDE

In Appendix B, from Eqs. (4.13) and (4.14) we have derived a compound asymptotic expression, which describes the relaxation kinetics in the whole region BCDE:

$$\xi_{1,0} = \left(\frac{\tau_{DE}}{\pi\tau}\right)^{1/2} + \left(\frac{\tau_{BC}}{\pi\tau}\right)^{1/2} \exp\left(-\frac{\tau}{\tau_C}\right) \tag{4.28}$$

$$(\tau > \tau_B; \beta >> 1)$$

For large τ, the exponential function is zero, and Eq. (4.28) reduces to Eq. (4.25) (regime DE). For $\tau/\tau_C << 1$, the exponential function is equal to 1, and Eq. (4.28) reduces to Eq. (4.19) (regime BC), because $\tau_{BC} >> \tau_{DE}$. Finally, for intermediate values of τ, we have an exponential transition between the regimes BC and DE (Fig. 2):

$$\xi_{1,0} \approx \left(\frac{\tau_{BC}}{\pi\tau}\right)^{1/2} \exp\left(-\frac{\tau}{\tau_C}\right) \quad (\text{regime CD},\ \tau_C < \tau < \tau_D) \tag{4.29}$$

Note that in regime CD the relaxation kinetics is influenced by the rate constant of the slow micellar process, K_s, through τ_C; see Eq. (4.15).

Eq. (4.28) allows one to determine the time moment τ_D, i.e., the position of the point D, which represents the boundary between the regimes CD and DE (Fig. 2). Let us define τ_D as the value of τ, for which the two terms in the right-hand side of Eq. (4.28) are equal. Thus, we obtain:

$$\tau_D \equiv \tau_C \ln\left[\left(\frac{\tau_{BC}}{\tau_{DE}}\right)^{1/2} - 1\right] \approx 2\tau_C \ln\left(\frac{m_{eq}}{\sigma_{eq}}\right). \tag{4.30}$$

In Fig. 4 we compare the exact numerical solutions of the general system in Section 3.1, and of the simplified system, Eqs. (4.12)–(4.14). The three curves correspond to different values of K_m/K_s; the other parameters are given by Eq. (3.14). The curves calculated by using the general and the simplified systems of equations are in excellent agreement: they differ only for $\tau < \tau_B$ (on the left of the point B in Fig. 4), where the simplified system is not valid by presumption. For the same parameter values, we calculated $\xi_{1,0}(\tau)$ by using the compound asymptotic expression, Eq. (4.28). The results were practically identical with those obtained by numerical solution of the simplified system, Eqs. (4.12)–(4.14): the respective calculated curves coincide in Fig. 4. This confirms that Eq. (4.28) holds with high precision in the whole relaxation region BCDE.

The vertical dashed lines in Fig. 4 correspond to the time moment τ_D, calculated by means of Eq. (4.30) for each of the three curves in the figure. The respective three values, τ_{D1}, τ_{D2}, and τ_{D3}, mark the positions of the boundary points, D_1, D_2, and D_3, for the three curves.

4.6. Discussion: "fast" and "slow" surfactants and experimental methods

We will call "fast" surfactant an amphiphilic component, which adsorbs quickly at the interface. Likewise, a "fast" experimental method for dynamic surface tension measurement is a method, which allows one to detect early stages of the adsorption kinetics. Here the use of the terms "fast" and "slow" is relative: a method, which is "slow" for a given surfactant, could be "fast" for another surfactant.

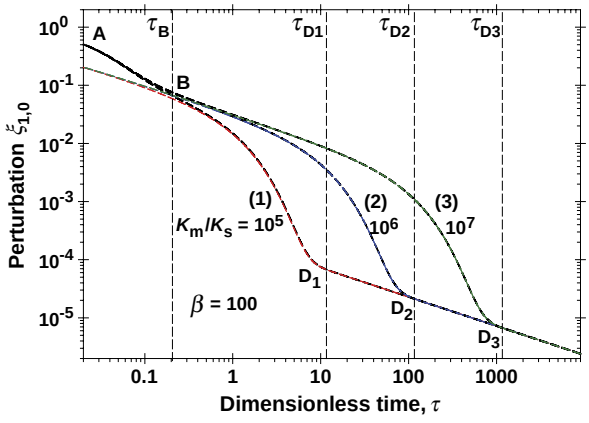

Fig. 4. Comparison of the simplified system, Eqs. (4.12)–(4.14), corresponding to diffusion affected by the slow relaxation process (the dashed lines), against the exact numerical solution of the general system in Section 3.1, the solid lines; $\beta = 100$. Each of the three curves corresponds to a fixed value of K_s/K_m denoted in the figure; the other parameters are given by Eq. (3.14). The values of τ_D, calculated from Eq. (4.30), correspond to the point D for the respective curves, 1, 2, and 3.

From this viewpoint, the initial stage of the adsorption kinetics from micellar solutions, the region AB in Fig. 2, could be registered for "slow" surfactants by "fast" methods. In contrast, the region BC in Fig. 2 could be registered for "fast" surfactants by "slow" methods. The regions CD and DE in Fig. 2 are difficult for detection because $\xi_{1,0}(\tau)$ is very small in these regions ($\xi_{1,0} \ll 1$ for $\tau > \tau_C$). In principle, the regions CD and DE could be detected for fast surfactants by slow and very sensitive methods. (In Section 5 we demonstrate that the regime DE is easier for detection in the case of "rudimentary" kinetic diagram, which could be observed at lower micelle concentrations, β, and greater values of the rate-constant, K_m, of the fast micellar process.)

At our best knowledge, until now the initial regime AB has been observed only for the nonionic surfactant Triton X-100 by means of the inclined plate method [14,19]. For the same surfactant, the data by the maximum-bubble-pressure method [13] correspond to the regime BC, although deviations from diffusion-limited adsorption has been observed at the greater frequencies (indications for the regime AB). Thus, it turns out that the inclined-plate method is faster than the maximum-bubble-pressure method. Of course, as mentioned above, the use of the terms "fast" and "slow" is relative here.

Another point, which deserves discussion, is the applicability of the assumption of small perturbation and, consequently, the limits of the developed model. Below the CMC, the conventional measurements of dynamic surface tension are often incompatible with this approximation and one has to take into account non-linear effects. However, for concentrations above the CMC, the situation is quite different. The characteristic time of the fast micellar process is so short that the micelles quickly damp any perturbation in the surfactant adsorption. For this reason, most of the experimental methods for interfacial dynamics (except the fastest ones) produce data in the regime of small deviations from equilibrium. This is confirmed by the good agreement of the developed theory (assuming small deviations) with experimental data obtained by various methods. For example, in [19] we have demonstrated that data from the inclined-plate method are in very good agreement with Eq. (4.7) (regime AB). In addition, in a subsequent paper [47], which could be considered as Part 3 of the present study, we demonstrate that Eq. (4.20) complies very well with data for the dynamic surface tension and adsorption produced by the strip method [12] and the overflowing cylinder method [20,27,48] (regime BC). The present theoretical approach could also find applications for interpretation of experimental results obtained by means of the maximum bubble pressure method [13], the fast-formed drop method [39,40], methods with oscillating surface area [2,3,49,50], etc.

5. Stages of a rudimentary kinetic diagram

5.1. Merged or missing regimes BC and CD

In Fig. 5 we present numerical results for $\xi_{1,0}(\tau)$, $\xi_{c,0}(\tau)$, $\xi_{m,0}(\tau)$, and $\xi_{\sigma,0}(\tau)$ obtained by solving the general system of equations in Section 3.1 by means of the numerical procedure described in Appendix A. In contrast with Fig. 2, the curves in Fig. 5 are calculated for a low micelle concentration, $\beta = 1$; i.e., the total surfactant concentration is $2 \times$ CMC, see Eq. (2.8). The perturbation $\xi_{\sigma,0}(\tau)$, which is similar for Fig. 5a, b and c, is shown only in Fig. 5a. As mentioned above, $\xi_{1,0}$ expresses not only the perturbation in the subsurface monomer concentration, but also the perturbations in the surface tension and adsorption, see Eq. (3.10).

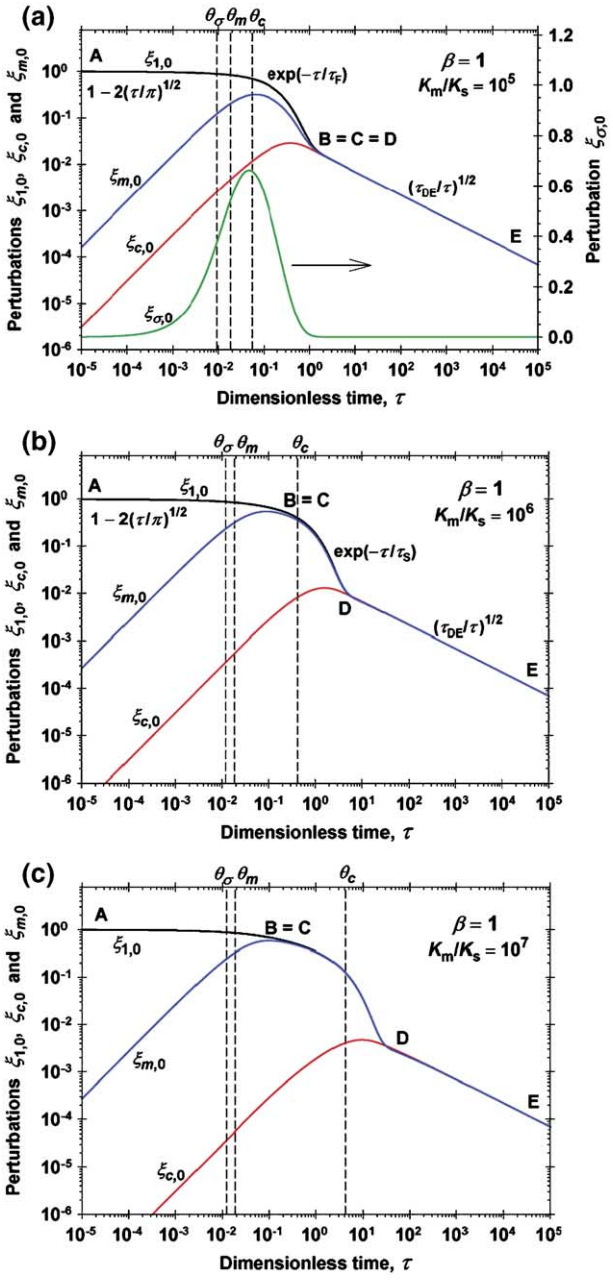

Fig. 5. Time dependence of the subsurface (at $z = 0$) perturbations in monomer concentration, $\xi_{1,0}$, micelle concentration, $\xi_{c,0}$, mean aggregation number, $\xi_{m,0}$, and polydispersity, $\xi_{\sigma,0}$, for $\beta = 1$; the other parameters are given by Eq. (3.14). The curves are obtained by exact numerical solution of the system of equations in Section 3.1. (a) $K_m/K_s = 10^5$; stages BC and CD are missing; (b) $K_m/K_s = 10^6$; missing stage BC; (c) $K_m/K_s = 10^7$; missing stage BC. Analytical expressions for the asymptotics of $\xi_{1,0}$ are shown in (a) and (b). $\xi_{\sigma,0}$, which is similar for (a), (b) and (c), is shown only in (a). θ_m, θ_σ and θ_c are the three characteristic micellization times (Table 1).

The most important difference between the relaxation curves in Figs. 5 and 2, is that the intermediate regimes BC and CD in Fig. 5 are merged or missing. Indeed, the point B has been defined as the point where $\xi_{m,0}$ and $\xi_{1,0}$ merge, while the point D marks the merging of $\xi_{c,0}$ and $\xi_{1,0}$. In Fig. 5a, the points B and D coincide, which means that the whole region BCD is missing in this kinetic diagram. In Fig. 5b and c, the points B and D are distinct, but there is no region BC in which $\xi_{1,0} \propto \tau^{-1/2}$; see Section 4.3 above. Hence, the point C cannot be defined as the boundary between regimes of inverse-square-root and exponential relaxation; see Fig. 2c. It turns out that the whole region BCD in Fig. 5b and c can be described by an integral expression, Eq. (5.6). Such kinetic diagrams (Fig. 5), in which the intermediate stages BC and CD are merging or missing, will be termed *rudimentary* kinetic diagrams.

On the other hand, the initial and final stages, AB and DE, are always present in the kinetic diagrams, both "regular" (Fig. 2) and "rudimentary" (Fig. 5). The analytical expressions for $\xi_{1,0}(\tau)$ at these stages are the same as given in Sections 4.1 and 4.4, irrespective of whether the diagram is regular or rudimentary. In particular, the short-time asymptotics, $\xi_{1,0} = 1 - 2(\tau/\pi)^{1/2} + \ldots$, given by Eq. (4.6), is valid in all cases.

In general, Fig. 5 illustrates that the increase of the ratio K_m/K_s may lead to a transition from rudimentary to regular kinetic diagram. Another parameter, whose variation may induce such transition, is the rate constant of the fast micellar process, K_m. In Fig. 6 we show six relaxation curves, $\xi_{1,0}(\tau)$, each of them corresponding to different K_m. The curves 1 and 2 exhibit rudimentary relaxation pattern; the curve 3 is transitional, while the curves 4, 5 and 6 have regular relaxation pattern. The boundaries of the separate stages are denoted by A, B_4, C_4 and D_4 for the curve 4 (Fig. 6). The point D is well distinct for each curve and is denoted by $D_1, \ldots, D_6$. Thus, the curves in Fig. 6 indicate that the increase of K_m (at fixed other parameters) may induce a transition from regular to rudimentary kinetic diagrams.

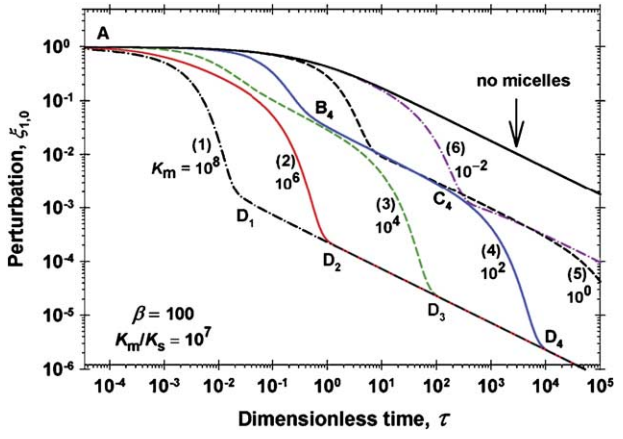

Fig. 6. Plot of the perturbation in the subsurface monomer concentration, $\xi_{1,0}$, vs. time for $\beta = 100$ and $K_s/K_m = 10^7$. Each of the six curves corresponds to a fixed value of K_m denoted in the figure; the other parameters are given by Eq. (3.14). The curves are obtained by exact numerical solution of the general system of equations in Section 3.1. For curves 1 and 2 the relaxation pattern is rudimentary (the stages BC and CD are missing or merging). For curves 4, 5 and 6 the relaxation pattern is regular, with separate stages AB, BC, CD, and DE. The curve 3 is transitional between regular and rudimentary relaxation.

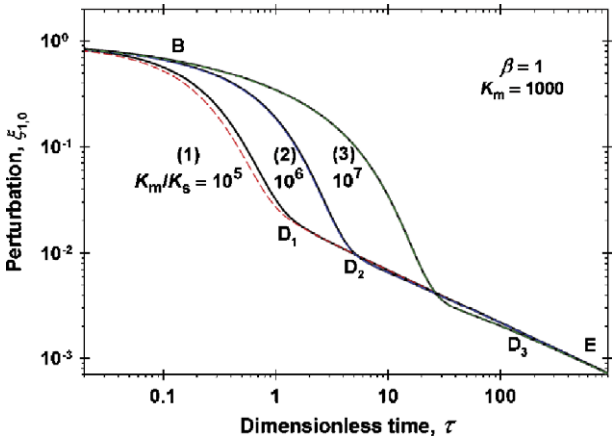

Fig. 7. Comparison of the solution of the simplified boundary problem, Eqs. (4.12)–(4.14), the dashed lines, against the exact numerical solution of the general system in Section 3.1, the solid lines. The perturbation in the subsurface concentration of monomers, $\xi_{1,0}$, is plotted vs. time for $\beta = 1$ and $K_m = 1000$. Each of the three curves corresponds to a fixed value of K_s/K_m denoted in the figure; the other parameters are given by Eq. (3.14).

In addition, the family of curves in Fig. 6 exhibits three asymptotes, representing straight lines of slope $-1/2$, and corresponding to diffusion-limited adsorption. The upper asymptote corresponds to micelle free solution; the intermediate asymptote corresponds to the regime BC, and the lower asymptote corresponds to the regime DE.

5.2. Description of the region BCD for rudimentary diagrams

The whole relaxation curve, ABCDE in Figs. 2 and 5, can be described by solving numerically the general system of equations in Section 3.1. Alternatively one could describe the whole region BCDE by numerically solving the simpler system of Eqs. (4.13) and (4.14), along with the boundary condition, Eq. (4.12). In Fig. 7, the continuous lines $\xi_{1,0}(\tau)$ are computed from the general equations in Section 3.1, while the dashed lines are calculated by solving numerically Eqs. (4.12)–(4.14). The dashed and continuous curves practically coincide for curves 2 and 3, for which $K_m/K_s = 10^6$ and 10^7 (corresponding to Fig. 5b and c). In contrast, for $K_m/K_s = 10^5$, that is curve 1 in Fig. 7, such excellent agreement is missing. The reason is that for curve 1 we have a broad region with $\xi_{m,0}(\tau) \ll \xi_{1,0}(\tau)$ (region AB in Fig. 5a), while the simplified system of Eqs. (4.12)–(4.14) is based on the assumption that $\xi_{m,0}(\tau) \approx \xi_{1,0}(\tau)$. Note also that in the case of rudimentary kinetic diagrams, Eq. (4.30) cannot be used to determine the positions of the point D on the diagram.

Analytical expression for the region BCD of a rudimentary kinetic diagram (Fig. 5b and c) can be derived in the following way. We have $\xi_{c,0} \ll \xi_{1,0}$ everywhere in the region BCD, except the vicinity of the point D (see Fig. 5b and c). Consequently, for this region we can neglect ξ_c in Eq. (4.13):

$$\left(1 + \frac{\beta\sigma_{eq}^2}{m_{eq}S}\right)\frac{\partial\xi_1}{\partial\tau} = \left(1 + \frac{\beta\sigma_{eq}^2}{m_{eq}S}B_m\right)\frac{\partial^2\xi_1}{\partial\zeta^2} - \frac{m_{eq}^2 K_s}{S}\xi_1 \tag{5.1}$$

The boundary condition for Eq. (5.1) is given by Eq. (4.12). The resulting problem is equivalent to the known pseudo-first-order-reaction (PFOR) approximation. Let us formally introduce new dimensionless variables:

$$\hat{\zeta} \equiv \left(1 + \frac{\sigma_{eq}^2 \beta}{m_{eq} S}\right) \zeta, \quad \hat{\tau} \equiv \tau / \tau_{BC} \tag{5.2}$$

where τ_{BC} is defined by Eq. (4.18). Then, Eqs. (5.1) and (4.12) acquire the form:

$$\frac{\partial \xi_1}{\partial \hat{\tau}} = \frac{\partial^2 \xi_1}{\partial \hat{\zeta}^2} - \frac{1}{\tau_S} \xi_1 \tag{5.3}$$

$$\frac{\partial \xi_1}{\partial \hat{\tau}} = \frac{\partial \xi_1}{\partial \hat{\zeta}} \quad \text{at } \hat{\zeta} = 0 \text{ and } \hat{\tau} > 0 \tag{5.4}$$

where the characteristic time τ_S is defined as:

$$\tau_S \equiv \left(1 + \frac{\beta \sigma_{eq}^2}{m_{eq} S}\right)^2 \left(1 + \frac{\beta \sigma_{eq}^2}{m_{eq} S} B_m\right) \frac{S}{m_{eq}^2 K_s} \tag{5.5}$$

Eq. (5.3), along with Eq. (5.4), has a general integral solution, which is analogous to Eq. (4.4):

$$\xi_{1,0}(\hat{\tau}) = \frac{s_B - 1}{s_B} \exp\left(-\frac{s_B - 1}{2} \hat{\tau}\right) + \frac{2}{\pi} \int_0^\infty \exp\left[-\left(\frac{1}{\tau_s} + \tau^2\right) \hat{\tau}\right] \times \frac{\tau^2}{\left(\tau^2 + 1/\tau_S\right)^2 + \tau^2} d\tau \tag{5.6}$$

where

$$s_B \equiv \left(1 + \frac{4}{\tau_S}\right)^{1/2} \tag{5.7}$$

The asymptotics of Eq. (5.6) for large $\hat{\tau}$ is [19]:

$$\xi_{1,0} = \frac{s_B - 1}{s_B} \exp\left(-\frac{s_B - 1}{2} \hat{\tau}\right) + \cdots (\text{for} \exp(-\hat{\tau}/\tau_S) << 1) \tag{5.8}$$

In particular, for $4/\tau_S << 1$, we have $(s_{B-1})/2 \approx 1/\tau_S$. Then, Eq. (5.8) reduces to:

$$\xi_{1,0} \approx \frac{2}{\tau_S} \exp\left(-\frac{\hat{\tau}}{\tau_S}\right) + \cdots \left(\text{for} \frac{4}{\tau_S} << 1\right) \tag{5.9}$$

Thus, the region BCD contains a sub-domain with exponential decrease of $\xi_{1,0}(\tau)$ (see Fig. 5b and c). In this sub-domain, $\xi_{1,0}$ decreases much faster than the slower square root decay in the region DE. For smaller values of $\hat{\tau}$ (closer to the point B), the asymptotic formula, Eq. (5.8), could become inapplicable, and then one should use the more general Eq. (5.6).

6. Summary and conclusions

In this paper, the set of equations obtained in [1] is applied for theoretical modeling of surfactant adsorption from micellar solutions after a small initial perturbation of the interface. The proposed model gives a general picture of the interfacial relaxation kinetics, including the variation of the adsorption and interfacial tension; see Section 3 and Fig. 2. The derived general system of kinetic equations (Section 3.1) describes all stages of the relaxation process at both high and low micelle concentrations; for both "fast" and "slow" surfactants and experimental methods; for arbitrary values of all parameters of the micellar system.

The following kinetic regimes (stages) have been identified (Fig. 2): AB–exponential asymptotics governed by the fast micellization process (Section 4.1); BC–inverse-square-root asymptotics: equilibrated fast process but negligible slow process, and diffusion limited kinetics (Section 4.3); CD–exponential asymptotics governed by the slow micellization process (Section 4.5), and DE–inverse-square-root asymptotics: both the fast and slow micellization processes are equilibrated and the kinetics is diffusion-limited (Section 4.4).

Regime AB can be detected by fast methods; for example, Triton X-100 by the inclined plate method [14,19]. Regime BC can be detected by slower methods; for example, Triton X- 100 by the maximum-bubble pressure method [13]. Regimes CD and DE are difficult for detection because the decaying perturbation, $\xi_{1,0}(\tau)$, has become very small for these regimes (Fig. 2); in principle, regimes CD and DE could be detected for fast surfactants by slow and sensitive methods.

Rudimentary kinetic pattern is observed at low micelle concentration ($\beta \approx 1$, Fig. 5) and/or at sufficiently great values of K_m, the rate constant of the fast micellization process (Fig. 6). Merging or missing of the kinetic regimes BC and CD characterizes such rudimentary diagrams (Section 5).

From the viewpoint of applications, the developed theoretical model could help the experimentalists to identify the kinetic regime for each specific surfactant solution detected by a given experimental method. The model provides theoretical expressions for data processing in each separate regime. The characteristic relaxation times of the various regimes, such as τ_F, τ_C, τ_{BC}, τ_{DE} and τ_S, turn out to be the same, irrespective of the used experimental method. In other words, Eqs. (4.5) (4.15) (4.18) (4.24) and (5.5) have a general validity. On the other hand, the derived equations for the time dependence of surface tension, $\xi_{1,0}(\tau)$, in different regimes are specific to the type of the used method, in our case, relaxation of a quiescent interface after an initial perturbation. The application of the present theoretical approach to other classes of dynamic methods (with stationary and non-stationary interfacial dilatation, and with oscillating surface area) will be subjects of subsequent studies.

Acknowledgement

This work was supported by Unilever Research US, Trumbull, CT.

Appendix A. Procedure for solving the general system in Section 3

The linear system of Eqs. (3.3)–(3.6), with boundary condition (3.11), is solved numerically as follows. First

Laplace transform, L, is applied; the respective Laplace images are:

$$\tilde{\xi}_1 \equiv L[\xi_1], \tilde{\xi}_c \equiv L[\xi_c], \tilde{\xi}_m \equiv L[\xi_m], \tilde{\xi}_\sigma \equiv L[\xi_\sigma] \quad (A.1)$$

Below, the parameter of the Laplace transform will be denoted by q. The Laplace images of the diffusion Eqs. (3.3)–(3.6), written in a matrix form, are:

$$\frac{d^2\tilde{\xi}_i}{d\zeta^2} = a_{ij}\tilde{\xi}_j \quad (i,j = 1,c,m,\sigma) \quad (A.2)$$

where the coefficients a_{ij} are:

$$a_{11} = q + \left(m_{eq} - w\sigma_{eq}\right)^2\frac{K_s}{S} + \frac{\beta K_m}{m_{eq}S},$$
$$a_{1c} = -m_{eq}\left(m_{eq} - w\sigma_{eq}\right)\frac{K_s}{S} \quad (A.3)$$

$$a_{1m} = w\sigma_{eq}\left(m_{eq} - w\sigma_{eq}\right)\frac{K_s}{S} - \frac{\beta K_m}{m_{eq}S},$$
$$a_{1\sigma} = -\left(w^2-1\right)\left(m_{eq} - w\sigma_{eq}\right)\frac{K_s}{S} + \frac{\beta K_m}{\sigma_{eq}^2 m_{eq}S} \quad (A.4)$$

$$a_{c1} = -\left(m_{eq} - w\sigma_{eq}\right)\frac{K_s}{\beta B_m},\ a_{cc} = \frac{q}{B_m} + \frac{m_{eq}K_s}{\beta B_m} \quad (A.5)$$

$$a_{cm} = -w\sigma_{eq}\frac{K_s}{\beta B_m},\ a_{c\sigma} = \left(w^2-1\right)\frac{K_s}{\beta B_m} \quad (A.6)$$

$$a_{m1} = \left(m_{eq} - w\sigma_{eq}\right)\frac{K_s}{B_m}\frac{wm_{eq}}{\beta\sigma_{eq}} - \frac{K_m}{B_m\sigma_{eq}^2},$$
$$a_{mc} = -m_{eq}\frac{K_s}{B_m}\frac{wm_{eq}}{\beta\sigma_{eq}} \quad (A.7)$$

$$a_{mm} = \frac{q}{B_m} + w\sigma_{eq}\frac{K_s}{B_m}\frac{wm_{eq}}{\beta\sigma_{eq}} + \frac{K_m}{B_m\sigma_{eq}^2},$$
$$a_{m\sigma} = -\left(w^2-1\right)\frac{K_s}{B_m}\frac{wm_{eq}}{\beta\sigma_{eq}} - \frac{K_m}{B_m\sigma_{eq}^4} \quad (A.8)$$

$$a_{\sigma 1} = -\left(w^2-1\right)\left(m_{eq} - w\sigma_{eq}\right)\frac{K_s}{B_m}\frac{m_{eq}}{2\beta} + \frac{K_m}{2B_m\sigma_{eq}^2},$$
$$a_{\sigma c} = m_{eq}\left(w^2-1\right)\frac{K_s}{B_m}\frac{m_{eq}}{2\beta} \quad (A.9)$$

$$a_{\sigma m} = -w\sigma_{eq}\left(w^2-1\right)\frac{K_s}{B_m}\frac{m_{eq}}{2\beta} - \frac{K_m}{2B_m\sigma_{eq}^2} \quad (A.10)$$

$$a_{\sigma\sigma} = \frac{q}{B_m} + \left(w^2-1\right)^2\frac{K_s}{B_m}\frac{m_{eq}}{2\beta} + \frac{K_m\left(1+4\sigma_{eq}^2\right)}{2B_m\sigma_{eq}^4} \quad (A.11)$$

To find the solution of the linear system of Eq. (A.2), all eigenvalues of this system have to be calculated. For that reason, the solution is assumed proportional to $\exp(-\lambda\zeta)$. The latter expression is substituted into Eq. (A.2) and the characteristic equation $\det(a_{ij} - \lambda^2\delta_{ij}) = 0$ is obtained, where δ_{ij} is the Kronecker delta. For calculation of the four complex eigenvalues, λ_k^2, and the components of the eigenvectors, f_{ik} ($k = 1,c,m,\sigma$), we used the QZ algorithm, described in [51,52]. The complex value of λ_k is chosen in such a way that $\mathrm{Re}(\lambda_k) > 0$. Thus, the solution of the system (A.2) can be presented in the form:

$$\tilde{\xi}_i = \sum_{k=1,c,m,\sigma} f_{ik}X_k\exp(-\lambda_k\zeta) \quad (i = 1,c,m,\sigma) \quad (A.12)$$

where the unknown constants, X_k, are determined from the boundary conditions. With the help of the Laplace transform, Eq. (A.1), the boundary conditions (3.11) are represented in the form:

$$q\tilde{\xi}_1 - \frac{d\tilde{\xi}_1}{d\zeta} = 1,\ \frac{d\tilde{\xi}_c}{d\zeta} = \frac{d\tilde{\xi}_m}{d\zeta} = \frac{\tilde{\xi}_\sigma}{d\zeta} = 0 \,(\text{at } \zeta = 0) \quad (A.13)$$

where the initial condition, Eq. (3.12), has been also used. After substitution of Eq. (A.12) into the boundary conditions, Eq. (A.13), one obtains the following linear system of equation for X_k:

$$\sum_{k=1,c,m,\sigma}(q\delta_{1i} + \lambda_k)f_{ik}X_k = \delta_{1i} \quad (i = 1,c,m,\sigma) \quad (A.14)$$

The linear complex system of Eqs. (A.14) is solved using the LU factorization method; see [53]. We are interested in the values of the perturbations at the interface ($\zeta = 0$), where Eq. (A.12) acquires the form:

$$\tilde{\xi}_{i,0} = \sum_{k=1,c,m,\sigma} f_{ik}X_k \quad (i = 1,c,m,\sigma) \quad (A.15)$$

The inverse Laplace transformation of Eq. (A.15) is performed by numerical inversion, using a Fourier series approximation; see [54,55].

Appendix B. Solution of the diffusion problem in Section 4

To find the exact solution of the boundary problem (4.12)–(4.14), we will use Laplace transform with respect to time; see Eq. (A.1). The Laplace images of Eqs. (4.13) and (4.14) are:

$$\left(1 + \frac{\beta\sigma_{eq}^2}{m_{eq}S}\right)q\tilde{\xi}_1 = \left(1 + \frac{\beta\sigma_{eq}^2}{m_{eq}S}B_m\right)\frac{d^2\tilde{\xi}_1}{d\zeta^2} - \frac{m_{eq}^2K_s}{S}\left(\tilde{\xi}_1 - \tilde{\xi}_c\right) \quad (B.1)$$

$$q\tilde{\xi}_c = B_m\frac{d^2\tilde{\xi}_c}{d\zeta^2} + \frac{m_{eq}K_s}{\beta}\left(\tilde{\xi}_1 - \tilde{\xi}_c\right) \quad (B.2)$$

(q is the Laplace parameter). The initial conditions are given by Eqs. (3.12) and (3.13), while the boundary conditions are Eq. (4.12) and $\partial\xi_c/\partial\zeta = 0$ at $\zeta = 0$. Their Laplace transforms are:

$$q\tilde{\xi}_1 - 1 = \left(1 + \frac{\beta\sigma_{eq}^2}{m_{eq}S}B_m\right)\frac{d\tilde{\xi}_1}{d\zeta} \text{ at } \zeta = 0 \text{ and } \tau > 0 \quad (B.3)$$

$$\frac{d\tilde{\xi}_c}{d\zeta} = 0 \text{ at } \zeta = 0 \text{ and } \tau > 0 \tag{B.4}$$

Let λ_1 and λ_2 be the characteristic values of the system of differential Eqs. (B.1) and (B.2), chosen in such a way that $\lambda_1>0$ and $\lambda_2>0$. Then the Laplace transforms of ξ_1 and ξ_c are obtained in the form:

$$\tilde{\xi}_c = \frac{\tilde{\xi}_{c,0}}{\lambda_2 - \lambda_1}[\lambda_2 \exp(-\lambda_1\zeta) - \lambda_1 \exp(-\lambda_2\zeta)] \tag{B.5}$$

$$\begin{aligned}\tilde{\xi}_1 = {} & \frac{\tilde{\xi}_{c,0}}{(\lambda_2-\lambda_1)\left(q + m_{eq}K_s\right)/\beta + B_m\lambda_1\lambda_2)} \\ & \times \left[\left(q + m_{eq}K_s\right)/\beta - B_m\lambda_1^2\right)]\lambda_2 \exp \\ & \times (-\lambda_1\zeta) - \left(q + m_{eq}K_s/\beta - B_m\lambda_2^2\right)\lambda_1\exp(-\lambda_2\zeta)].\end{aligned} \tag{B.6}$$

Here, $\tilde{\xi}_{c,0}$ and $\tilde{\xi}_{1,0}$ are the values of ξ_c and ξ_1 at $\zeta=0$. Note that Eqs. (B.5) and (B.6) satisfy the diffusion Eqs. (B.1) and (B.2), and the boundary condition (B.4). The substitution of Eq. (B.6) into the second boundary condition, Eq. (B.3), yields an expression for) $\tilde{\xi}_{1,0}(q)$:

$$\tilde{\xi}_{1,0} = \left[q + \frac{B_m\lambda_1\lambda_2(\lambda_1+\lambda_2)}{q + m_{eq}K_s/\beta + B_m\lambda_1\lambda_2}\left(1 + \frac{\sigma_{eq}^2\beta}{m_{eq}S}B_m\right)\right]^{-1} \tag{B.7}$$

Next, we have to determine $\lambda_1(q)$ and $\lambda_2(q)$. The characteristic equation for the system of Eqs. (B.1) and (B.2) represents a biquadratic equation: $a\lambda^4 - b\lambda^2 + c = 0$, where

$$a = \left(1 + \frac{\sigma_{eq}^2\beta}{m_{eq}S}B_m\right)B_m \tag{B.8a}$$

$$\begin{aligned}b(q) = {} & q + \frac{m_{eq}K_s}{\beta} \\ & + \left[\left(1 + \frac{2\sigma_{eq}^2\beta}{m_{eq}S}\right)q + \left(m_{eq}^2 + \sigma_{eq}^2\right)\frac{K_s}{S}\right]B_m\end{aligned} \tag{B.8b}$$

$$c(q) = \left[\left(1 + \frac{\sigma_{eq}^2\beta}{m_{eq}S}\right)q + m_{eq}\frac{K_s}{\beta} + \left(m_{eq}^2 + \sigma_{eq}^2\right)\frac{K_s}{S}\right]q \tag{B.8c}$$

With the help of the Viète's formulas we obtain:

$$\lambda_1^2 + \lambda_2^2 = b/a \tag{B.9}$$

$$\lambda_1\lambda_2 = (c/a)^{1/2} \tag{B.10}$$

and then we can determine

$$\lambda_1 + \lambda_2 = \left(\lambda_1^2 + \lambda_2^2 + 2\lambda_1\lambda_2\right)^{1/2} \tag{B.11}$$

The substitution of Eqs. (B.10) and (B.11) into Eq. (B.7), along with Eqs. (B.8a) (B.8b) (B.8c) and (B.9), gives the explicit dependence $\tilde{\xi}_{1,0}(q)$. We performed the inverse Laplace transformation of Eq. (B.7) by means of numerical inverse Laplace transform using a Fourier series approximation; see [54,55].

In the case of high surfactant concentrations, a simple asymptotic expression for $\xi_{1,0}(\tau)$ can be derived. For this goal, we first simplify Eqs. (B.1) and (B.2) for $\beta\sigma_{eq}^2/(m_{eq}S)>>1$:

$$q\tilde{\xi}_1 = B_m\frac{d^2\tilde{\xi}_1}{d\zeta^2} - \frac{m_{eq}^3K_s}{\sigma_{eq}^2\beta}\left(\tilde{\xi}_1 - \tilde{\xi}_c\right) \tag{B.12}$$

$$q\tilde{\xi}_c = B_m\frac{d^2\tilde{\xi}_c}{d\zeta^2} + \frac{m_{eq}K_s}{\beta}\left(\tilde{\xi}_1 - \tilde{\xi}_c\right) \tag{B.13}$$

The elimination of the last term in Eqs. (B.12) and (B.13) yields:

$$q\left(\tilde{\xi}_1 + \frac{m_{eq}^2}{\sigma_{eq}^2}\tilde{\xi}_c\right) = B_m\frac{d^2}{d\zeta^2}\left(\tilde{\xi}_1 + \frac{m_{eq}^2}{\sigma_{eq}^2}\tilde{\xi}_c\right) \tag{B.14}$$

The exact solution of Eq. (B.14) is:

$$\tilde{\xi}_1 + \frac{m_{eq}^2}{\sigma_{eq}^2}\tilde{\xi}_c = Y_1\exp\left[-\left(\frac{q}{B_m}\right)^{1/2}\zeta\right] \tag{B.15}$$

where Y_1 is a constant of integration. Note that in the left-hand side of Eq. (B.15) we have a multiplier $m_{eq}^2/\sigma_{eq}^2>>1$. Nevertheless, in the region BC we have $\tilde{\xi}_1>>\tilde{\xi}_c$, and the term $\tilde{\xi}_1$ could prevail in the left-hand side of Eq. (B.15). On the other hand, in the region DE we have $\tilde{\xi}_1\approx\tilde{\xi}_c$, and then the second term in the left-hand side of Eq. (B.15) becomes larger.

At the next step, we subtract equation (B.13) from equation (B.12):

$$q\left(\tilde{\xi}_1 - \tilde{\xi}_c\right) = B_m\frac{d^2}{d\zeta^2}\left(\tilde{\xi}_1 - \tilde{\xi}_c\right) - \frac{1}{\tau_C}\left(\tilde{\xi}_1 - \tilde{\xi}_c\right) \tag{B.16}$$

where

$$\frac{1}{\tau_C} \equiv \left(\frac{m_{eq}^2}{\sigma_{eq}^2} + 1\right)\frac{m_{eq}K_s}{\beta} \tag{B.17}$$

The solution of Eq. (B.16) is:

$$\tilde{\xi}_1 - \tilde{\xi}_c = Y_2\exp\left[-\left(\frac{q + 1/\tau_C}{B_m}\right)^{1/2}\zeta\right] \tag{B.18}$$

where Y_2 is a constant of integration. In the region BC, where $\tilde{\xi}_1>>\tilde{\xi}_c$, the first term in the left-hand side of Eq. (B.18) prevails, while in the region DE we have $\tilde{\xi}_1\approx\tilde{\xi}_c$.

Next, we eliminate $\tilde{\xi}_1$ between Eqs. (B.15) and (B.18) and substitute the result for $\tilde{\xi}_c$ into the boundary condition, Eq. (B.4); thus we find a relationship between Y_1 and Y_2:

$$Y_2 = Y_1\left(\frac{q}{q + 1/\tau_C}\right)^{1/2} \tag{B.19}$$

From Eqs. B.15), (B.18) and (B.19, we derive:

$$\tilde{\xi}_1 = \frac{Y_1}{1+v}\left\{\exp\left[-\left(\frac{q}{B_m}\right)^{1/2}\zeta\right] + \left(\frac{q}{u}\right)^{1/2}v\exp\left[-\left(\frac{u}{B_m}\right)^{1/2}\zeta\right]\right\} \tag{B.20}$$

where $u=q+1/\tau_C$ and $v=m_{eq}^2/\sigma_{eq}^2$. Using the relationship $\tilde{\xi}_1|_{\zeta=0}=\tilde{\xi}_{1,0}$, we further determine Y_1 in Eq. (B.20):

$$\tilde{\xi}_1=\tilde{\xi}_{1,0}\left[1+\left(\frac{q}{u}\right)^{1/2}v\right]^{-1}\left\{\exp\left[-\left(\frac{q}{B_m}\right)^{1/2}\zeta\right]+\left(\frac{q}{u}\right)^{1/2}\times v\exp\left[-\left(\frac{u}{B_m}\right)^{1/2}\zeta\right]\right\} \tag{B.21}$$

For large surfactant concentrations, Eq. (B.3) reduces to

$$q\tilde{\xi}_1-1=\frac{\beta\sigma_{eq}^2}{m_{eq}S}B_m\frac{d\tilde{\xi}_1}{d\zeta}\quad\text{at }\zeta=0\text{ and }\tau>0 \tag{B.22}$$

Substituting the solution (B.21) into the boundary condition (B.22), we get:

$$q\tilde{\xi}_{1,0}-1=-\frac{\beta\sigma_{eq}^2}{m_{eq}S}(B_mq)^{1/2}\left[1+\left(\frac{q}{u}\right)^{1/2}v\right]^{-1}(1+v)\tilde{\xi}_{1,0} \tag{B.23}$$

For $v>>1$, the latter equation reduces to:

$$\left\{q+\frac{m_{eq}\beta}{S}(B_mq)^{1/2}\left[1+\left(\frac{m_{eq}^2}{\sigma_{eq}^2}\right)\left(\frac{q}{q+1/\tau_C}\right)^{1/2}\right]^{-1}\right\}\tilde{\xi}_{1,0}=1 \tag{B.24}$$

Because the long-time limit, $\tau>>1$, corresponds to $q<<1$, from Eq. (B.24) we obtain the following asymptotic expression:

$$\tilde{\xi}_{1,0}=\left(\frac{\tau_{DE}}{q}\right)^{1/2}+\left(\frac{\tau_{BC}}{q+1/\tau_C}\right)^{1/2} \tag{B.25}$$

where

$$\frac{1}{\tau_{BC}}\approx\left(\frac{\sigma_{eq}^2\beta}{m_{eq}S}\right)^2B_m,\quad\frac{1}{\tau_{DE}}\approx\left(\frac{m_{eq}\beta}{S}\right)^2B_m \tag{B.26}$$

is the asymptotic form of Eqs. (4.18) and (4.24) for $\beta>>1$. Finally, the inverse Laplace transform of Eq. (B.26) yields Eq. (4.28); see e.g., [46].

References

[1] Danov KD, Kralchevsky PA, Denkov ND, Ananthapadmanabhan KP, Lips A. Mass transport in micellar surfactant solutions: 1. Relaxation of micelle concentration, aggregation number and polydispersity. Adv Colloid Interface Sci in press. doi:10.1016/j.cis.2005.09.002.

[2] Lucassen J. Adsorption kinetics in micellar systems. Faraday Discuss Chem Soc 1975;59:76–87.

[3] Lucassen J, Giles D. Dynamic surface properties of nonionic surfactant solutions. J Chem Soc Faraday Trans I 1975;71:217–32.

[4] Miller R. Adsorption kinetics of surfactants from micellar solutions. Colloid Polym Sci 1981;259:1124–8.

[5] Fainerman VB. Kinetics of the adsorption of surfactants from micellar solutions (theory). Kolloidn Zh 1981;43:94–100.

[6] Fainerman VB, Rakita YM. Investigation of the dissociation kinetics of micelles from the dynamic surface tension of the expanding surface of micellar solutions. Kolloidn Zh 1981;43:106–11.

[7] Fainerman VB, Makievski AV. Study of micelle dissociation kinetics by dynamic surface tension of micellar solutions. Colloids Surf 1993;69:249–63.

[8] Dushkin CD, Ivanov IB. Effects of the polydispersity of diffusing micelles on the dynamic surface elasticity. Colloids Surf 1991;60:213–33.

[9] Dushkin CD, Ivanov IB, Kralchevsky PA. The kinetics of the surface tension of micellar surfactant solutions. Colloids Surf 1991;60:235–61.

[10] van Hunsel J, Bleys G, Joos J. Adsorption kinetics at the oil/water interface. J Colloid Interface Sci 1986;114:432–41.

[11] Joos P, van Hunsel J. Adsorption kinetics of micellar Brij 58 solutions. Colloids Surf 1988;33:99–108.

[12] Li B, Joos P, van Uffelen M. Adsorption kinetics of Brij 58 micellar solution. J Colloid Interface Sci 1995;171:270–5.

[13] Makievski AV, Fainerman VB, Joos P. Dynamic surface tension of micellar Triton X-100 solutions by the maximum-bubble-pressure method. J Colloid Interface Sci 1994;166:6–13.

[14] Geeraerts G, Joos P. Dynamic surface tension of micellar Triton X-100 solutions. Colloids Surf, A Physicochem Eng Asp 1994;90:149–54.

[15] Joos P. Dynamic surface phenomena. AH Zeist, The Netherlands: VSP BV; 1999.

[16] Noskov BA, Grigoriev DO. Adsorption from micellar solutions. In: Fainerman VB, Möbius D, Miller R, editors. Surfactants: chemistry, interfacial properties, applications. Amsterdam: Elsevier; 2001. p. 401–509.

[17] Noskov BA. Kinetics of adsorption from micellar solutions. Adv Colloid Interface Sci 2002;95:237–93.

[18] Danov KD, Vlahovska PM, Horozov T, Dushkin CD, Kralchevsky PA, Mehreteab A, et al. Adsorption from micellar surfactant solutions: nonlinear theory and experiment. J Colloid Interface Sci 1996;183:223–35.

[19] Danov KD, Valkovska DS, Kralchevsky PA. Adsorption relaxation for nonionic surfactants under mixed barrier-diffusion and micellization-diffusion control. J Colloid Interface Sci 2002;251:18–25.

[20] Breward CJW, Howell PD. Straining flow of a micellar surfactant solution. Eur J Appl Math 2004;15:511–31.

[21] De Groot SR, Mazur P. Non-equilibrium thermodynamics. Amsterdam: North Holland; 1962.

[22] Van Voorst Vader F, Erkens ThF, van den Tempel M. Measurement of dilatational surface properties. Trans Faraday Soc 1964;60:1170–7.

[23] Edwards DA, Brenner H, Wasan DT. Interfacial transport processes and rheology. Boston: Butterworth-Heinemann; 1991.

[24] Ivanov IB, Danov KD, Ananthapadmanabhan KP, Lips A. Interfacial rheology of adsorbed layers with surface reaction: on the origin of the dilatational surface viscosity. Adv Colloid Interface Sci 2005;114–115:61–92.

[25] Kralchevsky PA, Radkov YS, Denkov ND. Adsorption from surfactant solutions under diffusion control. J Colloid Interface Sci 1993;161:361–5.

[26] Breward CJW, Darton RC, Howell PD, Ockendon JR. The effect of surfactants on expanding free surfaces. Chem Eng Sci 2001;56:2867–78.

[27] Howell PD, Breward CJW. Mathematical modeling of the overflowing cylinder experiment. J Fluid Mech 2003;474:275–98.

[28] Baret JF. Theoretical model for an interface allowing a kinetic study of adsorption. J Colloid Interface Sci 1969;30:1–12.

[29] Dukhin S, Kretzschmar G, Miller R. Dynamics of adsorption at liquid interfaces. Amsterdam: Elsevier; 1995.

[30] Eastoe J, Dalton JS. Dynamic surface tension and adsorption mechanisms of surfactants at the air–water interface. Adv Colloid Interface Sci 2000;85:103–44.

[31] Diamant H, Andelman D. Kinetics of surfactant adsorption at fluid–fluid interfaces. J Phys Chem 1996;100:13732–42.

[32] Fainerman VB, Zholob SA, Miller R, Joos P. Non-diffusional adsorption dynamics of surfactants at the air/water interface: adsorption barrier or non-equilibrium surface layer. Colloids Surf, A Physicochem Eng Asp 1998;143:243–9.

[33] Danov KD, Kralchevsky PA, Ivanov IB. Equilibrium and dynamics of surfactant adsorption monolayers and thin liquid films. In: Broze G, editor. Handbook of detergents. Part. A: properties. New York: Marcel Dekker; 1999. p. 303–418.

[34] Kralchevsky PA, Nagayama K. Particles at fluid interfaces and membranes. Amsterdam: Elsevier; 2001. p. 48–53. Chapter 1.3.3.

[35] Passerone A, Liggieri L, Rando N, Ravera F, Ricci E. A new experimental method for the measurement of the interfacial tensions between

immiscible fluids at zero bond number. J Colloid Interface Sci 1991;146:152–62.
[36] Nagarajan R, Wasan DT. Measurement of dynamic interfacial tension by an expanding drop tensiometer. J Colloid Interface Sci 1993;159:164–73.
[37] Liggieri L, Ravera F, Passerone A. Dynamic interfacial tension measurements by a capillary pressure method. J Colloid Interface Sci 1995;169:226–37.
[38] Ferrari M, Liggieri L, Ravera F. Adsorption properties of $C_{10}E_8$ at the water-hexane interface. J Phys Chem B 1998;102(51):10521–7.
[39] Horozov T, Arnaudov L. A novel fast technique for measuring dynamic surface and interfacial tension of surfactant solutions at constant interfacial area. J Colloid Interface Sci 1999;219:99–109.
[40] Horozov T, Arnaudov L. Adsorption kinetics of some polyethylene glycol octylphenyl ethers studied by the fast formed drop technique. J Colloid Interface Sci 2000;222:146–55.
[41] Rillaerts E, Joos P. Rate of demicellization from the dynamic surface tensions of micellar solutions. J Phys Chem 1982;86:3471–8.
[42] Johner A, Joanny JF. Block copolymer adsorption in a selective solvent: a kinetic study. Macromolecules 1990;23:5299–311.
[43] Kabalnov A, Weers J. Kinetics of mass transfer in micellar systems: surfactant adsorption, solubilization kinetics, and ripening. Langmuir 1996;12:3442–8.
[44] Jordan PC. Chemical kinetics and transport. New York: Plenum Press; 1979.
[45] Sutherland KL. The kinetics of adsorption at liquid surface. Aust J Sci Res 1952;A5:683–96.
[46] Korn GA, Korn TM. Mathematical handbook. New York: McGraw-Hill; 1968.
[47] Danov KD, Kralchevsky PA, Ananthapadmanabhan KP, Lips A. Micellar surfactant solutions: dynamics of adsorption at fluid interfaces subjected to stationary expansion. Colloids Surf A Physicochem Eng Asp in press.
[48] Manning-Benson S, Bain CD, Darton RC. Measurement of dynamic interfacial properties in an overflowing cylinder by ellipsometry. J Colloid Interface Sci 1997;189:109–16.
[49] Kovalchuk VI, Krägel J, Aksenenko EV, Loglio G, Liggieri L. Oscillating bubble and drop techniques. In: Möbius D, Miller R, editors. Novel methods to study interfacial layers. Amsterdam: Elsevier; 2001. p. 485–516.
[50] Kovalchuk VI, Krägel J, Makievski AV, Ravera F, Liggieri L, Loglio G, et al. Rheological surface properties of C_{12}DMPO solution as obtained from amplitude- and phase-frequency characteristics of an oscillating bubble system. J Colloid Interface Sci 2004;280:498–505.
[51] Moler C, Stewart GW. An algorithm for generalized matrix eigenvalue problems. SIAM J Numer Anal 1973;10:241–56.
[52] Garbow BS. CALGO Algorithm 535: Q.Z. The algorithm to solve the generalized eigenvalue problem for complex matrices. ACM Trans Math Softw 1978;4:404–10.
[53] Dongarra JJ, DuCroz J, Hammarling S, Duff I. A set of level 3 basic linear algebra subprograms. ACM Trans Math Softw 1990;16:1–17.
[54] Crump KS. Numerical inversion of Laplace transforms using a Fourier series approximation. J Assoc Comput Mach 1976;23:89–96.
[55] De Hoog FR, Knight JH, Stokes AN. An improved method for numerical inversion of Laplace transforms. SIAM J Sci Statist Comput 1982;3:357–66.